



Production, Manufacturing, Transportation and Logistics

The two-echelon capacitated electric vehicle routing problem with battery swapping stations: Formulation and efficient methodology

Wanchen Jie^a, Jun Yang^{b,*}, Min Zhang^c, Yongxi Huang^d^aSchool of Information Management and Engineering, Zhejiang University of Finance and Economics, No. 18 Xueyuan Street, Xiasha Higher Education Park, Hangzhou, China^bSchool of Management, Huazhong University of Science and Technology, No. 1037 Luoyu Road, Wuhan, China^cSchool of Information Management, Wuhan University, Wuhan, China^dAmazon.com Inc., 333 Boren Ave. N, Seattle, WA 98109, United States

ARTICLE INFO

Article history:

Received 27 March 2017

Accepted 2 July 2018

Available online 8 July 2018

Keywords:

Routing

Two-echelon system

Electric vehicle city logistics

Column generation

Adaptive large neighborhood search

ABSTRACT

In this paper, we present a two-echelon capacitated electric vehicle routing problem with battery swapping stations (2E-EVRP-BSS), which aims to determine the delivery strategy under battery driving range limitations for city logistics. The electric vehicles operating in the different echelons have different load capacities, battery driving ranges, power consumption rates, and battery swapping costs. We propose an integer programming formulation and a hybrid algorithm that combines a column generation and an adaptive large neighborhood search (CG-ALNS) to solve the problem. We conducted extensive computational experiments, demonstrate the applicability of the proposed model, and show the efficiency of the CG-ALNS algorithm. In addition, we explore the interplay between battery driving range and the effectiveness of vehicle emission reduction through sensitivity analysis.

© 2018 Elsevier B.V. All rights reserved.

1. Introduction

There are a series of studies called “Green Logistics” whose aim is to increase the sustainability of transportation by considering the environmental and social issues. The usage of electric vehicles (EVs) instead of fossil fuel-based internal combustion vehicles (ICVs) is an important area of these Green Logistics studies. For example, the United States Environment Protection Agency and the National Highway Traffic Safety Administration are taking coordinated steps to enable the production of a new generation of clean vehicles, from the smallest cars to the largest trucks, to reduce greenhouse gas emissions and improve fuel use (NHTSA, 2016). The European Commission supports an urban e-mobility project called FREVUE, which seeks to demonstrate how EVs can meet the growing need for sustainable urban logistics (FREVUE, 2016). A delivery pattern of the Distripolis case in FREVUE is an example of a two-echelon transportation system. If the weight of goods is less than 200 kilograms, these goods will be transported to the urban bases located close to the main retailing districts at first (first echelon). Then, clean and quiet vehicles such as electric trucks are used for the second echelon to complete the final delivery. In accordance with the development tendency, EVs will be used more and

more widely in future transportation systems. Taking into consideration the external cost of logistics associated mainly with air pollution and noise, many logistics companies have introduced EVs for their operations. In 2010, FedEx announced that it would expand its alternative-energy vehicle fleet with the first all-electric FedEx parcel delivery trucks in the United States. The electric trucks began to join more than 1800 alternative-energy vehicles already in service for FedEx around the world (FedEx, 2010; Golson, 2014). In autumn 2015, UPS announced that it would deploy 18 electric, zero-emission delivery vehicles in Texas, USA (UPS, 2015).

The two-echelon vehicle routing problem (2E-VRP) arises in two-echelon transportation systems, which is very relevant to the context of city logistics (Savelsbergh & Woensel, 2016). In this study, we specifically consider EVs in the two-echelon vehicle routing problem to increase the sustainability of transportation. In the system, the freight available in a depot is transported to the transfer stations, which we call satellites, by large EVs, and then small EVs are used to deliver the freight in the satellites to the customers. The EVs operating in the different echelons that have different battery driving ranges should visit battery swapping stations (BSSs) to swap their batteries before their battery power runs out. The battery swapping of EVs replaces the existing battery that is almost depleted by a fully charged one, which is a major and promising solution (Li, 2014). The whole operation time of battery swapping could take less than 10 minutes, which is much faster

* Corresponding author.

E-mail address: jun_yang@hust.edu.cn (J. Yang).

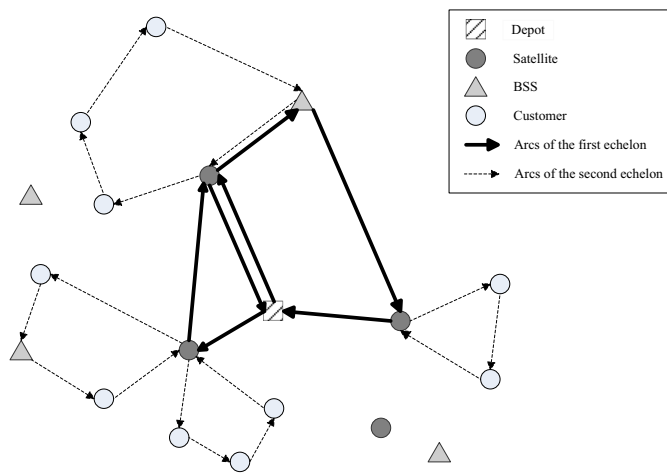


Fig. 1. An example of 2E-EVRP-BSS transportation network.

than battery recharging (Kim, 2011). Furthermore, depleted batteries of EVs can be charged during off-peak hours with a discounted electricity price. Owing to the limited driving range, routing and battery swapping are important to service customers promptly and fulfil orders. We name this problem as the two-echelon electric vehicle routing problem with battery swapping stations (2E-EVRP-BSS). The goal of the two-echelon EV transport system is to improve the efficiency of city logistics while keeping the emission under control.

The present paper examines the 2E-EVRP-BSS with heterogeneous EVs in different echelons. More specifically, this problem extends the traditional 2E-VRP incorporated with EV driving range limitations and battery swapping strategies. Instead of the traditional 2E-VRP, our problem considers the EVs of the first echelon to have large limited driving ranges and loading capacities, whereas the EVs of the second echelon have small limited driving ranges and loading capacities. The EVs of both echelons can share the same BSSs. All locations of depot, satellites, BSSs, and customers are given and fixed. Fig. 1 shows an example of the 2E-EVRP-BSS transportation network. Our proposed model for this problem is to determine (a) the utilization of satellites and the shipment transported to these satellites considering the loading capacity limitation, (b) the allocation of satellites or customers to EVs in each echelon, and (c) the route of each EV in both echelons with a visit to the BSSs to accomplish the delivery with sufficient energy. The contribution of the present work is multifold. First, our work is the first to study the 2E-EVRP-BSS and propose a corresponding model of the problem and provide the applicability of the examined model. Second, we propose a powerful algorithm called CG-ALNS, which is a combination of column generation (CG) and adaptive large neighborhood search (ALNS) to solve the 2E-EVRP-BSS. BSS and battery related operators are first created in the algorithm, which are been proved making important contributions to the algorithm. The performance of CG-ALNS was evaluated by a large number of computational experiments. Finally, we highlight the managerial implications of the interplay between battery driving ranges and the efficiency of vehicle emission reduction in the economic analysis. These insights may provide some decision and strategy support for a logistics corporation operating an EV transportation network.

The remainder of the paper is organized as follows. In Section 2, we review recent studies related to EV routing problems and two-echelon distribution systems. The 2E-EVRP-BSS mathematical model is presented in Section 3. In Section 4, we present the CG-ALNS algorithm and provide the details for solving the 2E-EVRP-

BSS. Section 5 presents the results of the computational experiments with an extensive analysis of the heuristics performance and the efficiency of vehicle emission reduction. We conclude this study and outline the potential future directions in Section 6.

2. Literature review

The 2E-EVRP-BSS primarily combines two streams of research. The first stream is related to the electric vehicle routing problem (EVRP), and the other stream involves the 2E-VRP.

Related papers on the EVRP

As EVs have gained in popularity worldwide over the past decade, the issues related to the usage of EVs for transportation have opened up a wide range of relevant research works. Pelletier, Jabali, and Laporte (2016) provided researchers with the technological and marketing background of goods distribution with EVs and presented a review of existing research works in the EVRP field. Their overview summarized the main existing research works on EVs in transportation science, which covers three parts: fleet size and mix, vehicle routing, and optimal paths. From their work, they found that EVs have many advantages such as frequent stop-and-go movements, low travel speeds and reduced pollution, and noise in last-mile deliveries of urban logistics.

Apart from the review of main existing research works on EVs in Pelletier et al. (2016), Desaulniers, Errico, Irnich, and Schneider (2016) studied four variants of the EV routing problem with time windows, which are classified by the allowed recharge times per route and battery charge strategy (full recharges or partial recharges). Yang and Sun introduced a BSS location routing problem with capacitated EVs, which focuses on simultaneously determining the location of BSSs and the routing plan of EVs under battery driving range constraints (Yang & Sun, 2015). Moreover, the basic model they formulated allowed a BSS to be visited at most once, whereas in their extended model a BSS can be visited several times. Schiffer and Walther (2017b) considered both partial and full recharging options for EVs in their location-routing model of recharging stations, as well as time window constraints. In their objective function, they minimized not only the travel distance, but also the number of EVs and the number of recharging stations. Adler and Mirchandani (2014) presented an online routing problem of EVs, which minimizes the average delay of all vehicles by occasionally detouring them for the benefit of future ones by making battery reservations. Liao, Lu, and Shen (2016) studied the EV touring problem. Their objective is to find the route with the shortest travel time for a given road network. In the route, an EV can travel between a pair of vertices or visit a set of vertices with several stops.

Exact algorithm was used to solve the EV routing problem with time windows. According to a set partitioning formulation and a labelling algorithm, Desaulniers et al. provided branch-price-and-cut algorithms to solve four variants of their problem optimally and found solutions for instances with up to 100 customers and 21 recharging stations. In literature, the EV related problems were solved mostly by heuristics. Hof, Schneider, and Goeke (2017) showed how to extend solution methods for vehicle routing problems with intermediate stops to solve the BSS location routing problem with capacitated vehicles. Their extended AVNS algorithm improved the previously known best solutions for the instances of Yang and Sun (2015), and proved robust with regard to its average solution quality. Schiffer and Walther (2017a) studied a location routing problem with intra-route facilities and proposed an adaptive large neighborhood search algorithm with dynamic programming for it. According to their paper, the methodology can solve various problems with intra-route facilities by obtaining new best-known solutions for Yang and Sun (2015) and Schiffer and Walther (2017b).

Related papers on the 2E-VRP

Cuda, Guastaroba, and Speranza (2015) reviewed the foremost related papers on two-echelon distribution systems at the time. In their survey, the two-echelon location routing problem (2E-LRP), the two-echelon vehicle routing problem (2E-VRP) and the truck and trailer routing problem (TTRP) were considered. They stated that the study on the research area was still relatively unexplored despite its importance in practical applications. Li, Zhang, Lv, and Chang (2016b) introduced a short-term tactical problem named the two-echelon time-constrained vehicle routing problem in linehaul-delivery systems. They also gave a relatively comprehensive review of the 2E-VRP, 2E-LRP and TTRP.

(i) The node sets of 2E-LRP are composed of potential locations for the depots, potential locations for the satellites, and the customers. In other words, the location of the depots and the satellites to use is not determined a priori. The 2E-LRP aims at minimizing the total system cost with locating a number of depots and/or satellites among candidate sites which have specific costs. Gonzalez-Feliu (2012), and Prodhon and Prins (2014) provided the reviews on the 2E-LRP.

To the best of our knowledge, the best performing exact algorithm for the 2E-LRP is the branch-and-cut algorithm (Contardo, Hemmelmayr, & Crainic, 2012). The 2E-LRP and its variants were usually solved by heuristic algorithms. Prodhon and Prins (2014) gathered the results obtained by state-of-the-art metaheuristics on four sets of 2E-LRP instances. The adaptive large neighborhood search has the best performance on Nguyen's, Boccia's and Boccia's 2E-LRP instances (Contardo et al., 2012), and the variable neighborhood search for the 2E-LRP with several plants has the best performance on Prodhon's 2E-LRP instances (Schwengerer, Pirkwieser, & Raidl, 2012).

(ii) The 2E-VRP can be regarded as a special case of the 2E-LRP where the location of the depots and the satellites to use is given. For reviews on the 2E-VRP, we refer to Gonzalez-Feliu (2011), and Cuda et al. (2015). Jacobsen and Madsen (1980) first applied the routing problem to a two-echelon system by considering the daily distribution of newspapers through transfer points. Crainic, Ricciardi, and Storchi (2009) formally defined the concept of a 2E-VRP, although the term 2E-VRP arose later in the literature. They introduced a variant of 2E-VRP with time-dependent, synchronized, multi-depot, multi-product and heterogeneous fleets of each echelon and time windows. The 2E-VRP was first introduced in Perboli, Tadei, and Vigo (2011). They provided a mathematical formulation for the 2E-VRP which is based on the flow of the freight of each arc. However, Jepsen, Spoorendonk, and Ropke (2013) pointed out that the upper bounds of the model introduced in Perboli et al. (2011) may not be correctly provided when the solution has more than two open satellites. Li, Yuan, Lv, and Chang (2016a) introduced a short-term tactical problem in linehaul-delivery systems considering carbon dioxide emissions, which named the two-echelon time-constrained vehicle routing problem. Their case study showed the applicability of the model to real-life problems. Grangier, Gendreau, Lehuédé, and Rousseau (2016) studied a variant of the 2E-VRP that integrates constraints arising in city logistics such as time window constraints, synchronization constraints, and multiple trips at the second level. Dellaert, Crainic, Van Woensel, and Saridarq (2016) studied 2E-VRP with time windows, and provided two path-based mathematical formulation of the problem. Anderluh, Hemmelmayr, and Nolz (2017) developed a two-echelon city distribution scheme with temporal and spatial synchronization between cargo bikes and vans. Li, Liu, Jian, and Lu (2018) introduced the two-echelon distribution system considering the real-time transshipment capacity varying, and proposed a mixed integer linear programming model for it.

Some exact algorithms were used to solve the 2E-VRP. Exact algorithms include those found in Jepsen et al. (2013),

Baldacci, Mingozzi, Roberti, and Calvo (2013), Santos, da Cunha, and Mateus (2013), and Santos, Mateus, and da Cunha (2014). The method introduced by Baldacci et al. (2013) is considered as the best exact algorithm for the 2E-VRP, outperforming other existing exact algorithms. However, most of the 2E-VRP was solved by heuristics. The main heuristic algorithms for the 2E-VRP include math-based heuristics (Perboli & Tadei, 2010; Perboli et al., 2011), clustering-based heuristics (Crainic, Mancini, Perboli, & Tadei, 2008), GRASP (Crainic, Mancini, Perboli, & Tadei, 2011; 2013) and large neighborhood-based heuristics (Breunig, Schmid, Hartl, & Vidal, 2016; Hemmelmayr, Cordeau, & Crainic, 2012). The large neighborhood-based heuristic introduced by Breunig et al. (2016) has the best performance among these heuristic algorithms.

(iii) In the TTRP, the transport vehicles may be a truck pulling a trailer (a complete vehicle) or a single truck, some customers can be served only by a single truck and others can be reached either by a truck or by a complete vehicle (Lin, Yu, & Chou, 2009). For review on the TTRP, we refer to Drexel (2013). The capacitated TTRP is the most studied member of the class of TTRPs (Caramia & Guerriero, 2010; Villegas, Prins, Prodhon, Medaglia, & Velasco, 2013; Villegas, Prins, Prodhon, & Velasco, 2011), and some specific variants have been investigated in the literature (Derigs, Pullmann, & Vogel, 2013). To the best of our knowledge, the best performing heuristic for the capacitated TTRP is the matheuristic introduced in Villegas et al. (2013). The summary of solution algorithms and maximum size instances in each paper on TTRPs can be find in Cuda et al. (2015).

The electric vehicle routing problem and the two-echelon networks have drawn attention for academic research and practical application in literature. We first study the two-echelon routing problem in the context of electric vehicles application. In this paper, we need to determine the routing and battery swapping plan of heterogeneous EVs in both echelons simultaneously while considering the different driving ranges. From the perspective of mathematical model, loops are not allowed in the 2E-VRP model of Perboli et al. (2011) and Jepsen et al. (2013). However, in our 2E-EVRP-BSS, the same BSS can be visited several times by one vehicle, which means loops are allowed in our model. Furthermore, battery swapping costs are considered in our objective function. These settings would make more sense for a real-world routing problem. In Section 3, the construction of mathematical model for the 2E-EVRP-BSS is showed in more detail. Constraints (4) and (15) are important constraints that allow visit loops. From the perspective of algorithm, large neighborhood-based heuristics and branch-and-price algorithm (a hybrid algorithm of branch and bound and column generation methods) have very good performance respectively, which are most popular algorithms to solve the EV routing problems and 2E-VRP in the literature. In consideration of their own advantages which fit into the two echelon transportation mode of 2E-EVRP-BSS, we proposed the hybrid algorithm combined ALNS and CG to solve the 2E-EVRP-BSS. In addition, according to the characteristics of this problem, several new operators are created in this algorithm. These new operators play an important role in the algorithm, which are proved in Section 5.

3. Model formulation

3.1. Problem description

In this paper, we study the 2E-EVRP-BSS, which considers the delivery of goods from a depot to the customers through a set of satellites by two types of EVs. The problem has a depot, a set of satellites, a set of customers with a given demand and a set of BSSs without any service capacity constraints for both types of EVs to share, and the locations of all these nodes are given and fixed. A large-capacity EV type with a large battery driving range

for the first echelon and a small-capacity EV type with a small battery driving range for the second echelon were considered. In the first echelon, goods are delivered from the depot to the satellites by large EVs. In the second echelon, goods are delivered from the satellites to the customers by small EVs. The BSSs can provide the battery swapping service for the two types of EVs, and this operation will generate battery swapping costs. We assume that the large EVs at the depot and the small EVs at the satellites have full battery power.

Each customer must be visited exactly once by a small EV. Additionally, there is no need to use all the satellites; therefore, a satellite has two states: used or unused. Unlike the customers, a satellite can be visited several times by different large EVs to meet the demand. The capacities of both EV types cannot be exceeded, and each used EV makes a single trip. The number of large EVs available at the depot and the number of small EVs available at each satellite are limited. The unit handling cost of each satellite is specific. The objective is to minimize the sum of the EV travel costs, the battery swapping costs and the handling costs at the satellites.

3.2. Model

In this section, we introduce a mathematical formulation of the 2E-EVRP-BSS. According to the definition of 2E-EVRP-BSS, the freight must be delivered from the depot v_0 to the customer set $V_c = \{v_{c_1}, v_{c_2}, \dots, v_{c_n}\}$. Let q_i be the demand of customer v_{c_i} . The number of available EVs of the first echelon at the depot is k^1 with the same given capacity Q^1 . The number of available EVs of the second echelon is k^2 , and each satellite V_{s_i} has k_s^2 vehicles. The capacity of the second echelon vehicles is Q^2 .

In our model, the cost of the logistics distribution by EVs includes three parts:

- (1) Battery swapping costs, c_b^1 and c_b^2 , for each echelon per time.
- (2) Costs of the arcs traveled by the EVs in both echelons, c_{ij}^1 and c_{ij}^2 , for each echelon per unit distance; e.g. arcs connecting the depot to the satellites and the satellites between them in the first echelon, and arcs connecting the satellites to the customers and the customers between them in the second echelon.
- (3) Handling cost of the loading and unloading operations at the satellites, h_s , per unit freight.

We define two sets of variables:

- (1) The first set is like the traditional variables of the 2E-VRP. x_{ijk} denotes whether arc (i, j) is traveled by the EV k at the first echelon. z_{ijsk} denotes whether arc (i, j) is traveled by the EV k from satellite s in the second echelon. t_i is the decision variable that connects the two echelons, which denotes the total demand delivered to satellite $i \in V_S$ of the first echelon and also denotes the total demand of the second echelon to be served by this satellite. w_{ik} is defined to control the amount of flow through the satellite $i \in V_S$ by EV k , f_{ijk}^1 and f_{ijsk}^2 are defined to control the amount of flow through the BSSs. f_{ijk}^1 and f_{ijsk}^2 are necessary here because they help us build a model that allows the same BSS to be visited several times by an EV, which we will specially discuss after we discuss the model.
- (2) The second set represents the specific variables for EVs. b_{ik}^{1+} , b_{ik}^{1-} , b_{isk}^{2+} and b_{isk}^{2-} specify the remaining battery power when EV k arrives at or leaves node i of the two echelons.

To help the reader, we summarize the definitions of the variables and parameters in Table 1.

$$\begin{aligned} \min \quad & \sum_{k \in K^1} \sum_{(i,j) \in A_1} c_{ij}^1 x_{ijk} + \sum_{k \in K^2} \sum_{s \in V_S} \sum_{(i,j) \in A_2} c_{ijsk}^2 + \sum_{s \in V_S} h_s t_s \\ & + \sum_{k \in K^1} \sum_{b \in V_B} \sum_{(b,j) \in A_1} c_b^1 x_{bjk} + \sum_{k \in K^2} \sum_{s \in V_S} \sum_{b \in V_B} \sum_{(b,j) \in A_2} c_b^2 z_{bjksk} \end{aligned} \quad (1)$$

subject to

$$\sum_{(i,j) \in A_1} x_{ijk} = \sum_{(i,j) \in A_1} x_{jik} \quad \forall i \in V_S \cup V_B, k \in K^1 \quad (2)$$

$$\sum_{(i,j) \in A_1} x_{ijk} \leq 1 \quad \forall i \in V_S, k \in K^1 \quad (3)$$

$$\sum_{(i,j) \in A_1} f_{ijk}^1 = \sum_{(i,j) \in A_1} f_{jik}^1 \quad \forall i \in V_B, k \in K^1 \quad (4)$$

$$w_{ik} = \sum_{(i,j) \in A_1} f_{jik}^1 - \sum_{(i,j) \in A_1} f_{ijk}^1 \quad \forall i \in V_S, k \in K^1 \quad (5)$$

$$f_{ijk}^1 \leq Q^1 x_{ijk} \quad \forall (i, j) \in A_1, k \in K^1 \quad (6)$$

$$\sum_{i \in V_S} w_{ik} \leq Q^1 \quad \forall k \in K^1 \quad (7)$$

$$\sum_{k \in K^1} w_{ik} = t_i \quad \forall i \in V_S \quad (8)$$

$$\sum_{k \in K^2} \sum_{s \in V_S} \sum_{(i,j) \in A_2} z_{ijsk} = 1 \quad \forall i \in V_C \quad (9)$$

$$\sum_{(i,j) \in A_2} z_{ijsk} = \sum_{(i,j) \in A_2} z_{jisk} \quad \forall i \in V_C, s \in V_S, k \in K^2 \quad (10)$$

$$\sum_{s \in V_S \setminus \{s\}} \left(\sum_{(s,j) \in A_2} z_{sjks} + \sum_{(i,s') \in A_2} z_{is'sk} \right) = 0 \quad \forall s \in V_S, s' \in V_S', k \in K^2 \quad (11)$$

$$\sum_{k \in K^2} \sum_{s \in V_S} z_{ss'sk} = 0 \quad (12)$$

$$\sum_{k \in K^2} \sum_{(s,j) \in A_2} z_{sjks} \leq k_s^2 \quad \forall s \in V_S \quad (13)$$

$$\sum_{s \in V_S} \sum_{k \in K^2} \sum_{(s,j) \in A_2} z_{sjks} \leq k^2 \quad (14)$$

$$\sum_{(i,j) \in A_2} f_{ijsk}^2 = \sum_{(i,j) \in A_2} f_{jisk}^2 - q_i \quad \forall i \in V_C \cup V_B, s \in V_S, k \in K^2 \quad (15)$$

$$f_{ijsk}^2 \leq Q^2 z_{ijsk} \quad \forall (i, j) \in A_2, s \in V_S, k \in K^2 \quad (16)$$

$$\sum_{k \in K^2} \sum_{(i,j) \in A_2} q_i z_{ijsk} = t_s \quad \forall s \in V_S \quad (17)$$

$$b_{ik}^{1-} = B^1 \quad \forall i \in V_B \cup \{v_0\}, k \in K^1 \quad (18)$$

$$b_{ik}^{1-} = b_{ik}^{1+} \quad \forall i \in V_S, k \in K^1 \quad (19)$$

$$b_{jk}^{1+} \leq b_{ik}^{1-} - h^1 d_{ij} x_{ijk} + B^1 (1 - x_{ijk}) \quad \forall (i, j) \in A_1, k \in K^1 \quad (20)$$

$$b_{isk}^{2-} = B^2 \quad \forall i \in V_S \cup V_B, s \in V_S, k \in K^2 \quad (21)$$

$$b_{isk}^{2-} = b_{isk}^{2+} \quad \forall i \in V_C, s \in V_S, k \in K^2 \quad (22)$$

Table 1
Variables and parameters of the 2E-EVRP-BSS model.

V_0	Depot, $V_0 = \{v_0\}$
V'_0	Dummy depot, $V'_0 = \{v'_0\}$
V_S	Set of satellites, $V_S = \{v_{s_1}, v_{s_2}, \dots, v_{s_n}\}$
V'_S	Set of dummy satellites corresponding to V_S , $V'_S = \{v'_{s_1}, v'_{s_2}, \dots, v'_{s_n}\}$
V_C	Set of customers, $V_C = \{v_{c_1}, v_{c_2}, \dots, v_{c_n}\}$
V_B	Set of battery swap stations (BSSs), $V_B = \{v_{b_1}, v_{b_2}, \dots, v_{b_n}\}$
A_1	Set of arcs in the first echelon, $A_1 = \{(i, j) i \in V_0 \cup V_B \cup V_S, j \in V_B \cup V_S \cup V'_0, i \neq j\}$
A_2	Set of arcs in the second echelon, $A_2 = \{(i, j) i \in V_S \cup V_B \cup V_C, j \in V_B \cup V_C \cup V'_S, i \neq j\}$
n_s, n_c, n_b	Number of satellites, customers, and BSSs, respectively
k^1, k^2	Number of the first-echelon and of the second-echelon EVs, respectively
k_s^2	Number of the second-echelon EVs starting from satellite s
K^1, K^2	Set of the first-echelon and set of the second-echelon EVs, respectively
c_{ij}^1, c_{ij}^2	Cost of the first-echelon EVs from i to j and that of the second-echelon EVs, respectively
c_b^1, c_b^2	Cost of battery swapping at the first echelon and the second echelon, respectively
h_s	The unit handling cost of freight in satellite s
Q^1, Q^2	Capacity of the EVs for the first echelon and the second echelon, respectively
B^1, B^2	Battery capacity of the EVs for the first echelon and the second echelon, respectively
h^1, h^2	Charge consumption rate of the EVs for the first echelon and the second echelon, respectively
d_{ij}	Distance between nodes i and j
q_i	Demand of vertex i
x_{ijk}	Binary decision variable indicating whether arc (i, j) is traveled by the electric vehicle k in the first echelon
z_{ijsk}	Binary decision variable indicating whether arc (i, j) is traveled by the electric vehicle k from satellite s in the second echelon
t_i	Decision variable specifying the total demand delivered from satellite $i \in V_S$ of the first echelon; it also denotes the total demand of customers to be served by this satellite of the second echelon
w_{ik}	Decision variable specifying the amount of freight delivered to satellite $i \in V_S$ by vehicle k
f_{ijk}^1	Decision variable specifying the remaining cargo on arrival at j from i by vehicle k of the first echelon
f_{ijsk}^2	Decision variable specifying the remaining cargo on arrival at j from i by vehicle k from satellite s in the second echelon
b_{ik}^{1+}	Specifies the remaining battery power when vehicle k arrives at i in the first echelon
b_{ik}^{1-}	Specifies the remaining battery power when vehicle k leaves i in the first echelon
b_{isk}^{2+}	Specifies the remaining battery power when vehicle k arrives at i from satellite s in the second echelon
b_{isk}^{2-}	Specifies the remaining battery power when vehicle k leaves i from satellite s in the second echelon

$$b_{jsk}^{2+} \leq b_{isk}^{2-} - h^2 d_{ij} z_{ijsk} + B^2 (1 - z_{ijsk}) \quad \forall (i, j) \in A_2, s \in V_S, k \in K^2 \quad (23)$$

$$x_{ijk} \in \{0, 1\} \quad \forall (i, j) \in A_1, k \in K^1 \quad (24)$$

$$z_{ijsk} \in \{0, 1\} \quad \forall (i, j) \in A_2, s \in V_S, k \in K^2 \quad (25)$$

$$w_{ik} \geq 0 \quad \forall i \in V_S, k \in K^1 \quad (26)$$

$$t_i \geq 0 \quad \forall i \in V_S \quad (27)$$

$$f_{ijk}^1 \geq 0 \quad \forall (i, j) \in A_1, k \in K^1 \quad (28)$$

$$f_{ijsk}^2 \geq 0 \quad \forall (i, j) \in A_2, s \in V_S, k \in K^2 \quad (29)$$

$$b_{ik}^{1+}, b_{ik}^{1-} \geq 0 \quad \forall i \in V_1, k \in K^1 \quad (30)$$

$$b_{isk}^{2+}, b_{isk}^{2-} \geq 0 \quad \forall i \in V_2, s \in V_S, k \in K^2 \quad (31)$$

Objective function (1) minimizes the total cost including the EV shipping cost of both echelons, the loading and unloading operation costs at the satellites, and the battery swapping costs at the BSSs. Constraints (2)–(29) can be divided into four groups: Constraints (2)–(8) control the flow of goods of the first echelon. Constraints (9)–(17) control the flow of goods of the second echelon. Constraints (18)–(23) control the battery power of the EVs in both echelons. Finally, nonnegative variables and binary decision variables are defined in constraints (24)–(31).

Constraints (2) and (10) ensure the flow conservation for the EVs at each satellite in the first echelon and for each customer

in the second echelon, respectively. Constraint (3) ensures that a large EV visits a satellite at most once. Constraints (4) and (15) are part of the constraints that guarantee that a BSS can be revisited more than once. Constraints (4) is for the first echelon, and constraint (15) is for the second echelon. Constraints (4) and (15) with $q_i = 0$ indicate that the sum of the remaining load of an EV entering a BSS is equal to the sum of the remaining load of an EV leaving a BSS, which not only keeps the vehicle capacity balance but also indicates that a BSS can be visited more than once by the same vehicle. Constraints (5) and (15) with $q_i \neq 0$ track the change in the remaining load level of an EV on the basis of the node sequence of satellites and customers, respectively. In this way, our model guarantees that an EV will never visit a satellite or a customer more than once. Constraints (6) and (16) are the cargo flow limitation. If $x_{ijk} = 1$, the maximal remaining load level f_{ijk}^1 is at most the full vehicle capacity Q^1 . Otherwise, $f_{ijk}^1 = 0$. If $z_{ijsk} = 1$, the maximal remaining load level f_{ijsk}^2 is at most Q^2 . Otherwise, $f_{ijsk}^2 = 0$. Constraint (7) ensures that the total cargo of large EVs will not exceed their capacities. Constraint (8) denotes the total shipment that is delivered to a satellite, and constraint (17) represents the total shipment that is delivered to the customers from the corresponding satellite. Constraints (8) and (17) connect the first echelon and the second echelon through the variable t_s , respectively. Constraint (9) ensures that each customer is visited only once. Constraint (11) eliminates the traffic between the satellites in the second echelon, which means that we cannot dispatch EVs among satellites. Constraint (12) eliminates the direct traffic between a satellite and its dummy satellite in the second echelon, in other words, these arcs should not exist. Constraints (13) and (14) restrict the number of total available small EVs at each satellite and in the second echelon, respectively.

Constraint (18) ensures that the battery power of a large EV is equal to B^1 when it departs from the depot or visits a BSS, and constraint (21) ensures that the battery power of a small EV

is equal to B^2 when it departs from a satellite or visits a BSS. Constraints (19) and (22) ensure that the battery power remains the same when an EV visits a satellite and a customer, respectively. Constraints (20) and (23) keep the balance of the battery power of the large EVs and small EVs arriving at node j from node i , respectively. They guarantee that every EV has sufficient battery power to visit the remaining satellites or customers and return to the depot or satellites. If node j is visited by vehicle k after node i ($x_{ijk} = 1$ or $z_{ijsk} = 1$), the maximum distance that the remaining battery power allows upon arriving at node j is reduced on the basis of the distance between node i and node j .

4. Solution method for the 2E-EVRP-BSS

Our 2E-EVRP-BSS is solved by the CG-ALNS hybrid heuristic algorithm. CG-ALNS applies CG to solve the first echelon, which has a small or a medium number of nodes, and uses ALNS to handle the second echelon, which has a larger number of nodes. The concrete implementation of CG-ALNS will be described in the following sections.

4.1. Overview of the algorithmic framework

For the first echelon of the 2E-EVRP-BSS, not all satellites need to be used and the demands of the satellites are unknown in the beginning. In addition, a satellite can be visited several times by different large EVs. These issues make it complex to solve the first echelon of the 2E-EVRP-BSS in the first place. On this occasion, our CG-ALNS starts obtaining one solution of the second echelon and then solves the first echelon on the basis of the result of the second echelon.

In the second echelon, the goods are delivered from the satellites to the customers. It can be considered as a multi-depot EV routing problem (MDEVRP) by regarding the satellites as “depots”. ALNS was first introduced by Ropke and Pisinger (2006a) for vehicle routing problems. Many research works (Laporte, Musmanno, & Vucaturro, 2010; Ribeiro & Laporte, 2012; Ropke & Pisinger, 2006a) have proved that it is successful in solving large-sized vehicle routing problems because it can provide a high diversity of solutions and improve them effectively through the use of removal and insertion operations. We applied ALNS to solve the MDEVRP in the second echelon. The solution of this part can assign each customer to one satellite for transportation service, and we call this as a customer-to-satellite assignment configuration.

In the first echelon, the goods are delivered from the depot to the satellites. On the basis of the customer-to-satellite assignment configuration generated by ALNS, we can obtain the states of the satellites (used or unused) and their demands. The decision in the first echelon can be considered as a split delivery EV routing problem (SDEVRP) when each satellite is regarded as a “customer” with the demands assigned from the second echelon. In reality, the number of satellites is not large, which is up to 15 in the literature of the 2E-VRP. CG (Desaulniers, Desrosiers, & Solomon, 2006; Jin, Liu, & Eksioglu, 2008) has been shown to be very useful in exact algorithms and has a great advantage in speed when applied to small-size routing problems. Therefore, we adopted CG to solve the SDEVRP in the first echelon.

Algorithm 1 presents the pseudocode of our CG-ALNS algorithm. During the search procedure, CG-ALNS allows infeasible solutions. At first, an initial solution S_0^2 for the second echelon is generated on the basis of sweep algorithm, which is described in Section 4.3. On the basis of the result of S_0^2 , we use CG, which is presented in Section 4.4, to calculate the initial solution S_0^1 for the first echelon. Then, the initial solution S_0 of the 2E-EVRP-BSS is composed of S_0^1 and S_0^2 .

Algorithm 1 The whole CG-ALNS algorithm.

Require: Data of depot, satellites, customers, BSSs and EVs;
Ensure: The best-found solution S^* of the 2E-EVRP-BSS;
1: Generate an initial solution S_0^2 for the second echelon by using the extended sweep algorithm (ESA);
2: On the basis of S_0^2 , generate an optimal solution S_0^1 for the first echelon by using CG;
3: Obtain the initial solution $S_0 = \{S_0^1, S_0^2\}$;
4: $S, S^* \leftarrow S_0$;
5: $iter \leftarrow 0, T \leftarrow O(S_0) \times P_{init}$;
6: **while** $iter < OUTER^{MAX}$ and $T > T_{min}$ **do**
7: $S' \leftarrow S$;
8: Call ALNS and CG to optimize S' ;
9: Call LBO to adjust the stations of S'
10: **if** $O(S') < O(S)$ **then**
11: $S \leftarrow S'$;
12: **else**
13: Create a random number $\gamma \in [0,1]$;
14: **if** $\gamma < e^{-(O(S')-O(S))/T}$ **then**
15: $S \leftarrow S'$;
16: **end if**
17: **end if**
18: **if** $O(S) < O(S^*)$ **then**
19: $S^* \leftarrow S$;
20: **end if**
21: $iter \leftarrow iter + 1, T \leftarrow T \times \tau$;
22: **end while**
23: Return S^*

Starting from S_0 , the core CG-ALNS procedure will be executed $OUTER^{MAX}$ times. We set $OUTER^{MAX} = 400$ here. In each iteration, CG-ALNS first calls ALNS to optimize the second echelon part of the solution S' , calls CG to update the first echelon part of S' , finally, uses the label-based BSS optimization algorithm (LBO) which is a contribution of this algorithm to reduce the total cost of each route by adjusting the usage of BSSs. $O(S)$, $O(S')$ and $O(S^*)$ denote the objective function values of the current solution S , the neighbor solution S' and the best-found solution S^* , respectively. In reference to some related works such as Yang and Sun (2015), our acceptance criterion of S' is based on simulated annealing (SA). The criterion accepts $O(S')$ when $O(S') < O(S)$. If $O(S') \geq O(S)$, the criterion accepts $O(S')$ with a probability $e^{-(O(S')-O(S))/T}$, where T denotes the current temperature and changes by multiplying with a cooling rate τ . We set the initial temperature in SA as $O(S_0) \times P_{init}$, P_{init} is the initial temperature control parameter of SA.

4.2. Penalized objective function

To ensure the diversity of the solution space, we allow infeasible solutions that violate the battery driving range constraints by using a penalized objective function during the search. An infeasible solution violating the battery driving range will generate a penalizing cost. Let s_i^1 denote the battery feasibility of node $i \in V^1$ in the first echelon, if $b_{ik}^{1+} < 0$, $s_i^1 = |b_{ik}^{1+}|$; otherwise, $s_i^1 = 0$. The definition of s_i^2 is similar to that of s_i^1 . M_1 and M_2 denote very large numbers (we set $M_1 = 1000$ and $M_2 = 5000$ in the computational experiments after several calculations), and Z stands for the original objective function. Then, the penalized objective function is shown as follows:

$$Z_{penalized} = Z + M_1 \sum_{i \in V^1} s_i^1 + M_2 \sum_{i \in V^2} s_i^2 \quad (32)$$

4.3. Preprocessing procedures and generation of the initial solution

In this step, some preprocessing procedures are used to improve the speed of the algorithm. Following the procedures in the previous literature as Schneider, Stenger, and Goeke (2014), we remove an arc (u, v) that may inevitably produce an infeasible solution with the following rules:

1. $u, v \in V_C \wedge q_u + q_v > Q^2$, which means arcs violate the capacity constraint of the second echelon.
2. $u, v \in V_S \wedge \forall i \in V_B \cup \{v_0\}, j \in V_B \cup \{v_0'\} \wedge h^1(d_{iu} + d_{uv} + d_{vj}) > B^1$, which means arcs violate the battery capacity constraints of the first echelon.
3. $u, v \in V_C \wedge \forall i \in V_B \cup V_S, j \in V_B \cup V_S' \wedge h^2(d_{iu} + d_{uv} + d_{vj}) > B^2$, which means arcs violate the battery capacity constraints of the first echelon.

Rule 1 removes an arc (u, v) that violates the capacity constraint of the second echelon. Rules 2 and 3 are helpful in removing arcs that violate the battery capacity constraints in the first and the second echelons, respectively.

To generate an initial solution of the vehicle routing problem (VRP), Gillett and Miller (1974) first introduced the sweep algorithm. They claimed that this algorithm produces results better than those produced by Clarke and Wright's (1964) savings approach and by Christofides and Eilon's (1969) approach. According to the previous analysis of our problem, the initial solution S_0 consists of two parts: S_0^1 for the first echelon and S_0^2 for the second echelon. First, the initial solution of the second echelon S_0^2 is created based on the sweep algorithm. The characteristics of the 2E-EVRP-BSS are taken into account and the satellites are been inserted into each cluster in a greedy way. Then, the initial solution of the first echelon S_0^1 is generated by CG, which is shown in Section 4.4.

4.4. Column generation in the first echelon

After the solution of the second echelon is obtained, the first echelon is considered as the SDEVRP. In the SDEVRP, the demand of each used satellite can be split and delivered by one or more large EVs. CG is proposed to solve the SDEVRP, and the details are shown in the following subsections. First, we build an arc flow model for the SDEVRP. Second, we use the Dantzig–Wolfe decomposition principle to reformulate the model and transform it into a master problem on the basis of the routes and a subproblem. Third, a dynamic programming algorithm is adopted to solve the subproblem and search the routes with a negative reduced cost. A branch scheme is designed to obtain the integral solution. The CG process is shown in Algorithm 2.

Algorithm 2 Column generation algorithm (CG).

Require: The solution S^2 of the second echelon;
Ensure: The solution S^1 of the first echelon;
1: Generate an initial route set R_0 on the basis of the data of S^2 ;
2: Create a search stack $SS \leftarrow \emptyset$, $SS \leftarrow SS \cup \{R_0\}$;
3: Create the optimal route set $R^* \leftarrow \emptyset$;
4: Create an upper bound limit $UB \leftarrow MAX_VALUE$;
5: **while** $SS \neq \emptyset$ **do**
6: $R \leftarrow pop(SS)$
7: **repeat**
8: Solve the master problem on the basis of R with a simplex algorithm;
9: Calculate the dual values π and use π to build the subproblem;
10: Call the dynamic programming algorithm to search the route set denoted by R' ;
11: $R \leftarrow R \cup \{R'\}$
12: **until** $R' = \emptyset$
13: Obtain the cost $C(R)$;
14: **if** $C(R) < UB$ **then**
15: **if** \exists fractional arc (i, j) **then**
16: Branch on arc (i, j) ;
17: Obtain two branching route sets R^0 and R^1 from R ;
18: $SS \leftarrow SS \cup \{R^0, R^1\}$;
19: **else**
20: $R^* \leftarrow R$, $UB \leftarrow C(R)$;
21: **end if**
22: **end if**
23: **end while**
24: Return R^*

4.4.1. The arc flow model for the SDEVRP

In this section, we build the arc flow model for the SDEVRP. The model is used for the Dantzig–Wolfe decomposition in Subsection 4.4.2. Using a concept called “k-split cycles”, the authors in Dror and Trudeau (1990), Dror and Trudeau (1989) and Desaulniers (2010) proposed a useful property of the optimal solution of the SDVRP, which states that “If the distances satisfy the triangle inequality, then there exists an optimal solution such that, for each pair of reverse arcs in $A(N)$, at most one of them is traversed”. The detailed explanation of this property can be found in Archetti, Bianchessi, and Speranza (2011). We denote the decision variable ω_{ik} as the quantity delivered by EV $k \in K^1$ to node $i \in V_S \cup V_B$, which is a non-negative integer variable. $\bar{q}_i = \min\{q_i, Q^1\}$ denotes the maximum quantity that can be delivered to node i by one large EV, and the demands of BSSs are set to 0. Our arc flow model for the SDEVRP is also formulated according to this property.

$$\min \sum_{k \in K^1} \sum_{(i,j) \in A_1} c_{ij}^1 x_{ijk} + \sum_{k \in K^1} \sum_{b \in V_B} \sum_{(b,j) \in A_1} c_b^1 x_{bjk} + \sum_{i \in V_S} h_i q_i \quad (33)$$

$$\sum_{k \in K^1} \omega_{ik} = q_i \quad \forall i \in V_S \cup V_B \quad (34)$$

$$\sum_{k \in K^1} (x_{ijk} + x_{jik}) \leq 1 \quad \forall (i, j) \in A_1 \quad (35)$$

$$0 \leq \sum_{k \in K^1} \sum_{j \in V_S \cup V_B} x_{0jk} \leq k^1 \quad (36)$$

$$\sum_{j \in V_S \cup V_B} x_{v_0, j, k} = 1 \quad \forall k \in K^1 \quad (37)$$

$$\sum_{(i,j) \in A_1} x_{ijk} - \sum_{(i,j) \in A_1} x_{jik} = 0 \quad \forall k \in K^1, i \in V_S \cup V_B \quad (38)$$

$$\sum_{i \in V_S \cup V_B} x_{i, v_0', k} = 1 \quad \forall k \in K^1 \quad (39)$$

$$\sum_{i \in V_S \cup V_B} \omega_{ik} \leq Q^1 \quad \forall k \in K^1 \quad (40)$$

$$\sum_{(i,j) \in A_1} x_{ijk} \leq \omega_{ik} \leq \bar{q}_i \sum_{(i,j) \in A_1} x_{ijk} \quad \forall k \in K^1, i \in V_S \cup V_B \quad (41)$$

constraints (18)–(20)

$$\omega_{ik} \geq 0, \text{ integer} \quad \forall k \in K^1, i \in V_S \cup V_B \quad (42)$$

$$x_{ijk} \in \{0, 1\} \quad \forall k \in K^1, (i, j) \in A_1 \quad (43)$$

Objective function (33) calculates the total cost of the first echelon, which contains the travel cost, the battery swapping cost and the handling cost of freight in each satellite. Constraint (34) makes sure that the total quantity delivered to each satellite $i \in V_S$ is equal to its demand q_i . Constraint (35) agrees with the property mentioned above. Constraint (36) makes sure that the number of used vehicles is nonnegative and does not exceed k^1 . Constraints (37)–(39) keep the flow balance of a route, which starts from node v_0 and ends at node v_0' for each vehicle. Constraint (40) denotes the capacity constraints of the vehicles of the first echelon. Constraint (41) ensures the consistency between variables x_{ijk} and variables ω_{ik} . Constraints (18)–(20) are the battery constraints of the first echelon. Finally, non-negativity, integer and binary requirements are given by constraints (42) and (43).

4.4.2. Dantzig–Wolfe decomposition

According to the Dantzig–Wolfe decomposition principle, it is assumed that all of the feasible vehicle routes are known in advance. Then, the SDEVRP is transformed to choose the best routing combination that can satisfy all the constraints and obtain the minimum cost. Therefore, a corresponding model called the master problem model has to be built on the basis of the feasible routes for obtaining the optimal combination. However, it is almost impossible for us to get all of the feasible routes when building the master problem model. According to the duality theory and the dual values of the master problem model, the routes with a negative reduced cost can optimize the objective value by adding them to the master problem model. A subproblem model is proposed to search the routes with a negative reduced cost. Each candidate route is added as a column in the model. The detailed description of the decomposition procedure is introduced in [Dantzig and Wolfe \(1960\)](#).

1) Master problem

In the master problem model, we define the delivery pattern as a path where all passed satellites receive either a delivery of \bar{q}_i unit or a delivery unit that is greater than 1 and less than \bar{q}_i . θ_r is defined as the number of EVs assigned to route $r \in R$. We used a concept called extreme delivery pattern, which was introduced in [Archetti et al. \(2011\)](#); it means that there is only one satellite at most in a path that can receive a partial delivery between 1 and \bar{q}_i in the optimal solution. The other sets and parameters of this subsection are defined as follows:

R	Set of all feasible routes, which start from v_0 and return to v'_0 .
$R^s \subseteq R$	Set of routes that visit just one satellite.
$R^m \subseteq R$	Set of routes that visit more than one satellite.
$c_r^1 = \sum_{(i,j) \in R} c_{ij}^1 + \sum_{b \in R \cup V_B} c_b^1 + \sum_{s \in R \cup V_S} h_s t_s$	Cost of route $r \in R$, including travel cost, battery swapping cost and handling cost of freight in a satellite.
b_{ijr}	Binary parameter equal to 1 if arc $(i, j) \in A_1$ is traversed by route $r \in R$ or equal to 0 otherwise.
ω_{ir}	Quantity delivered to satellite $i \in V_S$, $r \in R$.

The master problem is formulated as:

$$\min \sum_{r \in R} c_r^1 \theta_r \quad (44)$$

$$\sum_{r \in R} \omega_{ir} \theta_r = q_i \quad \forall i \in V_S \cup V_B \quad (45)$$

$$\sum_{r \in R} (b_{ijr} + b_{jir}) \theta_r \leq 1 \quad \forall (i, j) \in A_1 \quad (46)$$

$$0 \leq \sum_{r \in R} \theta_r \leq k^1 \quad (47)$$

$$\theta_r \in \{0, 1\} \quad \forall r \in R^m \quad (48)$$

$$\theta_r, \text{ integer} \quad \forall r \in R^s \quad (49)$$

Objective function (44) calculates the total cost of the first echelon, just like (33). Constraints (45), (46), and (47) have the same function as those of constraints (34), (35), and (36). Binary and integer requirements are given in (48) and (49).

2) Subproblem

On the basis of the duality theory, we obtain the subproblem to search the routes with a negative reduced cost. The subproblem model uses the variable x_{ij} as defined in the 2E-EVRP-BSS model introduced in [Section 3](#) without the index of vehicle k . $\omega_i = \sum_{r \in R} \omega_{ir}$ denotes the quantity delivered to satellite $i \in V_S$. Some additional parameters for the subproblem model are denoted as follows:

π_i	Dual variable of constraint (45) for satellite $i \in V_S$. If $i \in V_B$, $\pi_i = 0$.
ρ_{ij}	Dual variable of constraint (46) for $(i, j) \in A_1$, and $\rho_{ij} = \rho_{ji}$.
β	Dual variable of constraint (47).

Then, the subproblem can be formulated as follows:

$$\min \sum_{(i,j) \in A_1} (c_{ij}^1 - \rho_{ij}) x_{ij} - \sum_{i \in V_S} \omega_i \pi_i - \beta \quad (50)$$

$$\sum_{j \in V_B \cup V_S} x_{v_0, j} = 1 \quad (51)$$

$$\sum_{(i,j) \in A_1} x_{ij} - \sum_{(i,j) \in A_1} x_{ji} = 0 \quad \forall i \in V_S \cup V_B \quad (52)$$

$$\sum_{i \in V_B \cup V_S} x_{i, v'_0} = 1 \quad (53)$$

$$\sum_{i \in V_S} \omega_i \leq Q^1 \quad (54)$$

$$\sum_{(i,j) \in A_1} x_{ij} \leq \omega_i \leq \bar{q}_i \quad \sum_{(i,j) \in A_1} x_{ij} \quad \forall i \in V_S \quad (55)$$

Constraints (18)–(20) without the index of vehicles k

$$\omega_i \geq 0, \text{ integer} \quad \forall i \in V_S \quad (56)$$

$$x_{ij} \in \{0, 1\} \quad \forall (i, j) \in A_1 \quad (57)$$

Objective function (50) searches the routes with the minimum negative reduced cost. Constraints (51)–(57) are the same as constraints (37)–(43), but without the index of vehicle k .

4.4.3. Dynamic programming algorithm and branching scheme

The subproblem is modeled as an elementary shortest path problem with resource constraints (SPPRC) ([Feillet, Dejax, Gendreau, & Gueguen, 2010](#); [Irnich & Desaulniers, 2005](#)). When the search space is huge, it is cumbersome to find the candidate route paths. In the solution methods for the SPPRC, the most commonly used algorithm is the dynamic programming algorithm ([Desrochers, 1988](#)) and ([Desrochers & Soumis, 1988](#)). It can build new paths and extend these paths one by one to all feasible directions. We define an expanded graph $G' = (V', A')$. The vertex set V' includes the depot v_0 ; the dummy depot v'_0 ; the vertices v_g^i representing the used satellite i with demand quantity g ; $g = 1, \dots, \bar{q}_i$; and the BSSs. For each used satellite i , A' contains arcs (v_0, v_g^i) with cost $c_{0i} - \rho_{0i} - \pi_i g$, arcs $(v_{q_i}^i, v'_0)$ with cost $c_{i0} - \rho_{i0}$, arcs $(v_{q_i}^i, v_g^j)$ with cost $c_{ij} - \rho_{ij} - \pi_j g$ and null cost arcs $(v_g^i, v_{q_i}^i)$. In addition, we do not allow paths with cycles, and a path that travels one satellite many times is forbidden.

In the dynamic programming algorithm, a labelling algorithm and dominance rules are adopted to help the search process. We denote a label of vertex i as $L_i = (i, p, r, T, \lambda, C, Q)$, where p is the index for accessing the previous label, r is the remaining battery driving range, T is the vector for recording the visited satellites, λ is the number of split satellites visited along the path, C is the current cost of the path and Q is the quantity loaded on the vehicle when leaving the vertex. Through λ , we control the number of the split satellites on the path. The initial state is represented by the label $(s, -1, B^1, T[s] = 1, 0, 0, 0)$. When travelling the arc (i, j) , the path will create a new label from $L_i = (i, p, r, T, \lambda, C, Q)$ to $L_j = (j, p', r', T', \lambda', C', Q')$. Along arcs (v_0, v_g^i) , $(v_{q_i}^i, v_g^j)$ and $(v_{q_i}^i, v'_0)$, the extension rules are

$$r' = \begin{cases} B^1, & \text{if } j \in V_B \\ r - d_{ij} * h^1, & \text{otherwise} \end{cases} \quad (58)$$

$$T'[j] = 1 \quad (59)$$

$$\lambda' = \begin{cases} \lambda + 1, & \text{if } 1 < g < \bar{q}_j \\ \lambda, & \text{otherwise} \end{cases} \quad (60)$$

$$C' = \begin{cases} C + c_{ij}^1 - \rho_{ij} - \pi_j g, & \text{if } 1 < g < \bar{q}_j \\ C + c_{ij}^1 - \rho_{ij} - \pi_j \bar{q}_j, & \text{otherwise} \end{cases} \quad (61)$$

$$Q' = Q + g \quad (62)$$

If $r' \geq 0$, $T'[j] \neq 1$, $\lambda' \leq \text{MAX}_S$ and $Q' \leq Q^1$, L_j resulting from this extension is deemed feasible. MAX_S is the upper bound of the split satellites in one path. If L_j is infeasible, delete it. We can define a dominance rule of constraints (58) – (62): Label $L_i = (i, p, r, T, \lambda, C, Q)$ dominates $L'_i = (i, p', r', T', \lambda', C', Q')$ when $r \geq r'$, $\lambda \leq \lambda'$, $C \leq C'$ and $Q \leq Q'$. If L_i dominates L'_i and $L_i \neq L'_i$, then L'_i can be discarded. If $L_i = L'_i$, then discard one of them.

A path can be created by traversing in reverse direction the index p of labels associated with the ending depot v'_0 . The solution of the subproblem is the paths that have negative costs! In our CG algorithm, the dynamic programming process stops when the number of generated path results reaches the upper limit n . We set n to twice the number of nodes in the graph. On the basis of the result, the master problem model can calculate new dual values that can update the parameters of the subproblem. The iteration between the master problem model and the subproblem stops when no negative reduced column is found and the optimal value is obtained.

The optimal value of the linear relaxation obtained above may not satisfy the integrality of the solution. In that case, a branching scheme is needed to cut off the fractional part of the solution. However, the general idea behind an effective branching scheme that is related to the variables is not suitable here because it may create an endless loop. In that case, we use a branching scheme that is based on the arc use, which was introduced in Ryan and Foster (1981). Inspired by the four branching schemes described in Jin et al. (2008), we made some improvement on the branching rule related to the arc use. At first, the fractional solution based on the route is transformed into a fractional value of its corresponding arc. b_{rij} is denoted as the value of arc (i, j) in route r . We first select the fractional value b_{rij} with $\text{Max}\{b_{rij} - \lfloor b_{rij} \rfloor, r \in R\}$ and branch it to 0 and 1. When b_{rij} is branched to 0, arc (i, j) will be marked in the label algorithm to make sure that routes with arc (i, j) will not be generated in the next route search. When b_{rij} is branched to 1, the route set of the master problem model needs to delete the other routes that include arc (i, j) . Moreover, in the next route search of the label algorithm, route r with arc (i, j) will be added to a new route set first. Then, the cost of the arc c_{ij}^1 is set to a very large value to make sure that routes that travel on arc (i, j) will not be generated.

4.5. ALNS framework

The ALNS heuristic algorithm is an extension of the Large Neighborhood Search (LNS) heuristic introduced by Shaw (1998). It was first introduced by Ropke and Pisinger (2006a) to solve the pickup and delivery problem. After that, ALNS has been widely used to solve several variants of the vehicle routing problem. An overview of our ALNS process is given in Algorithm 3. The removal and insertion operators are chosen by a roulette wheel mechanism on the basis of their weights. The weights of the operators are updated according to their historical performance. CG is called to re-calculate the solution of the first echelon $S^{1'}$ after the solution of the second echelon $S^{2'}$ is obtained. Then, a new solution S' for

Algorithm 3 Adaptive large neighborhood search algorithm.

Require: A solution S_0 of the 2E-EVRP-BSS;
Ensure: An improved solution S^* of the 2E-EVRP-BSS;
1: Initialise the weights and scores of the removal and insertion operators
2: $S, S^* \leftarrow S_0$;
3: $iter \leftarrow 0, T \leftarrow O(S_0) \times P_{init}$;
4: **while** $iter < \text{INNER}^{\text{MAX}}$ **do**
5: $S' \leftarrow S$;
6: Get the solution $S^{2'}$ of the second echelon from S' ;
7: Choose and apply the removal operator on $S^{2'}$;
8: Choose and apply the insertion operator on $S^{2'}$;
9: Call CG to get the solution $S^{1'}$ on the basis of $S^{2'}$;
10: $S' \leftarrow \{S^{1'}, S^{2'}\}$;
11: **if** $O(S') < O(S)$ **then**
12: $S \leftarrow S'$;
13: **else**
14: Create a random number $r \in [0, 1]$;
15: **if** $r < e^{-(O(S') - O(S))/T}$ **then**
16: $S \leftarrow S'$;
17: **end if**
18: **end if**
19: **if** $O(S) < O(S^*)$ **then**
20: $S^* \leftarrow S$;
21: **end if**
22: Update the weights and scores of the removal and insertion operators
23: $iter \leftarrow iter + 1, T \leftarrow T \times \zeta$;
24: **end while**
25: Return S^*

the 2E-EVRP-BSS is created, and the acceptance mechanism of S' is based on SA, which is the same as in Section 4.1. The iteration of ALNS will be executed $\text{INNER}^{\text{MAX}} = 500$ times.

4.5.1. Removal and insertion operators

This subsection introduces the removal and insertion operators in our ALNS. The removal operators remove n_r customers in each iteration. $n_r = (\mu_1 + (\mu_2 - \mu_1) \times r) \times n_C$, where n_C is the number of customers in the graph, and $\mu_1, \mu_2 \in (0, 1)$, $\mu_1 \leq \mu_2$ and $r \in [0, 1]$ are randomly created parameters. There are two types of removal operators in our ALNS: the first one only affects the second echelon by removing n_r customers; the second one affects both echelons of the problem, by not only removing n_r customers of the second echelon, but also by changing the state of the satellites of the first echelon.

Removal operators:

We utilize the *random customer removal (RCR)* and related customer removal (ReCR) (Ropke & Pisinger, 2006a), *satellite closing (SC)*, *satellite opening (SO)*, *satellite swapping (SS)* and *random route removal (RRR)* operators (Hemmelmayr et al., 2012) presented in the literature. RCR selects n_r customers of the second echelon at random and removes them from the current solution, it then places them into the customer pool. ReCR aims at removing the customers that are similar to the customer that has been removed. SC randomly closes one of the used satellites, removes the customers that were assigned to the satellite and places them into the customer pool. SO randomly uses one of the closed (unused) satellites. n_r customers that are closest to the selected satellite are removed from their current route. SS aims at exchanging the usage states of two satellites under a certain probability. RRR randomly removes a route and places the corresponding customers into the customer pool.

BSS-Customer Route Removal (BCRR): This operator aims at removing routes that visit more BSSs and fewer customers, because these routes have less contribution to the solution and produce unnecessary expenses. We denote $\text{BCRR}_r = (n_C^r + \alpha n_B^r) / (n_C^r + n_B^r)$ to calculate the contribution of route r , where n_C^r and n_B^r denote the number of customers and BSSs in route r in the second echelon, respectively. α is a predefined parameter that controls the proportion of customers and BSSs in the removed route. BCRR_r is sorted in ascending order. The larger BCRR_r is, the lesser route r contributes

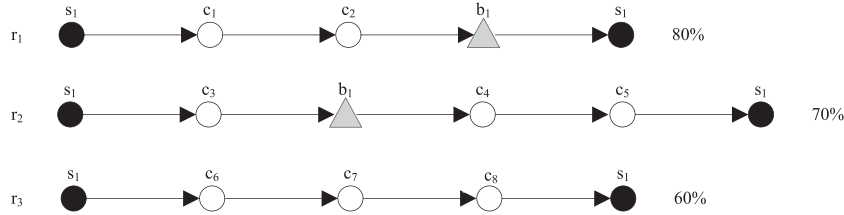


Fig. 2. Battery best use removal operator.

to the solution. This operator removes routes with the maximum value of $BCRR_r$ until n_r customers are removed.

BSS Proportion Route Removal (BPRR): This operator aims at removing routes that have a relatively large cost for visiting BSSs. We denote $BPRR_r = (\sum_{i \in V_B, j \in V_r} c_{ij} + \sum_{i \in V_r \setminus V_B, j \in V_B} c_{ij} + c_b^2 n_B^r) / c_r$ to calculate the proportion of BSS-related cost to the total cost of route r . V_r is denoted as the nodes in route r . n_B^r is denoted as in BCRR, and c_r denotes the total cost of route r of the second echelon. The larger $BPRR_r$ is, the larger the proportion of BSS-related cost to the total cost is. This operator removes routes with the maximum value of $BPRR_r$ until n_r customers are removed.

BSS Cost-Based Removal (BCBR): This operator aims at removing the customers that directly connect to a BSS with high travelling cost. The process helps find more suitable routes and BSSs for these removed customers. This operator first selects a BSS b at random. Then, the customer i that has the maximum value of c_{bi} or c_{ib} ($b \in V_B$) is removed. The process is repeated until n_r customers have been removed.

Battery Best Use Removal (BBUR): This operator aims at making sure that EVs use their batteries optimally. First, the operator selects the route r of the second echelon that returns to its satellite with the maximum value of the remaining battery driving range. Then, the customers between the satellite (terminal point of the second echelon) and the last BSS or the satellite (starting point of the second echelon) of r are removed. The process is repeated until n_r customers have been removed. For example, in Fig. 2, the right side denotes the remaining battery driving range of the EV in percentage form. According to BBUR, we choose route r_1 with 80% of battery driving range at first. However, there are no customers between the last BSS b_1 and s_1 . Therefore, route r_2 with 70% of battery driving range will be selected, and c_4 and c_5 between the last BSS b_1 and s_1 will be removed. If the number of removed customers is less than n_r , route r_3 with 60% of battery driving range will be selected, and c_6 , c_7 , and c_8 between s_1 (starting point) and s_1 (terminal point) will be removed.

Insertion operators:

The insertion operators are used to insert the removed customers back into the routes of the second echelon. In the process of insertion, we do not use the closed (unused) satellites but only consider the used ones.

Basic Greedy Insertion (BGI): We use the basic greedy insertion operator from the literature. In each iteration, this operator always inserts customers from the customer pool into its best position with the minimum insertion cost. The insertion cost is calculated by $Z_{cri} = c_{i-1,i}^2 + c_{i,i+1}^2 - c_{i-1,i+1}^2$ when inserting customer c into route r at position i . $Z_{cri} = +\infty$ when a customer c cannot be inserted into route r . The inserting customer c^* is selected as the one with the value $\min_{c \in Pool} \{\min_{r \in R'} \{\min_{i \in Pos} \{Z_{cri}\}\}\}$, where $Pool$ is the customer pool, R' is the route set of the second echelon after the removal operators are applied and Pos is the candidate position set in route r .

Basic Regret-K Insertion (BRKI*): Same as BGI, this operator is applied as done in the literature, but it prefers to insert the customers with the maximum regret value in the right position repeatedly, which aims to improve BGI using a type of look-ahead

mechanism when selecting a customer to insert (Pisinger & Ropke, 2007). The regret value is the sum of the cost differences among the top K best insertion positions, where K is a user-defined parameter and $K \geq 2$. Every time we choose the customer c^* with value $\max_{c \in Pool} \{\sum_{j=2}^K (Z_{cj} - Z_{c1})\}$ to insert. Z_{cj} represents the j th lowest insertion cost after customer c is reinserted into the solution. In our implementation, we just consider the situations of $K = 2$ and $K = 3$, which are named Basic Regret-2 Insertion (BR2I) and Basic Regret-3 Insertion (BR3I), respectively.

Advanced Greedy Insertion (AGI): After a customer is inserted, not only the travelling distance increases, but also the feasibility of the current solution will change. Unlike that in BGI, the insertion cost is changed to $Z_{cri} = \eta(c_{i-1,i}^2 + c_{i,i+1}^2 - c_{i-1,i+1}^2) + (1 - \eta)(\sum_{v \in V} s_c^2 - \sum_{v \in V'} s_c^2) + c_{penalty}$ when customer c is inserted in the i th position of route r , $\eta \in [0, 1]$ (Yang & Sun, 2015). s_c^2 represents the feasibility state of customer c that we already defined in Section 4.2. V and V' denote the vertex set of route r before and after the insertion, respectively. $c_{penalty} = M_c \max\{(\sum_{c \in r} q_c - Q^2), 0\}$ denotes the penalty of exceeding vehicle capacity, where M_c denotes a very large value. On the basis of the new calculation formula of the insertion cost, the operator prefers to select the best insertion that satisfies both the battery driving range limitation and the vehicle capacity constraints.

Advanced Regret-K Insertion (ARKI*): Customer $c = \arg \max_{c \in Pool} \{\sum_{j=2}^K (Z_{crj} - Z_{cr1})\}$ is selected by this operator to its best inserting position. ARKI is similar to BRKI, but it replaces the regret value with Z_{crj} . In our algorithm, we consider the situations of $K = 2$ and $K = 3$.

4.5.2. Adaptive selection of operators

In this section, we show the mechanism of the operator selection, which is based on the weights of the operators. In our ALNS, the weights of the operators are automatically adjusted according to their historical performance. We divide the search into a number of segments of 100 consecutive iterations, like what Ropke and Pisinger did in Ropke and Pisinger (2006a). The operators are selected by a roulette wheel mechanism in each iteration. Then, the selection probability of operator i in segment m is $p_{im} = w_i / \sum_{i \in OP} w_{im}$, where OP is the set of removal or insertion operators and w_{im} stands for the weight of the operator i in segment m . We set the initial value of weight $w_{init} = 0$. After 100 iterations, the weights of the operators are updated according to the score obtained during the segment. $w_{i,m+1} = \begin{cases} (1 - \theta) \times w_{im} + \theta \times \eta_{im} / N_{im}, & \text{if } N_{im} \neq 0 \\ w_{i,m}, & \text{otherwise} \end{cases}$, where θ is the reaction factor, N_{im} denotes the times operator i is used in segment m and η_{im} denotes the score of operator i in the m segment. We set $\eta_{im} = 0$ initially, and it increases on the basis of the historical performance of operator i at iteration h . If the new solution is a new best-found solution, σ_1 is added to the score; if it is a new improving solution, σ_2 is added; if it is an accepted deteriorating solution, σ_3 is added; otherwise, 0 is added.

4.6. Label-based BSS optimization algorithm

The aforementioned approaches primarily focus on the optimization of satellites and customers, but not on BSSs. Therefore, in this section, a label-based BSS optimization algorithm (LBO) is proposed to optimize the use of the BSSs for each route. Since the choices of many BSSs and the constraints of the battery driving range are considered, this problem is not simple to solve exactly with a dynamic programming approach or to find an approximate solution with a constrained shortest path algorithm. Therefore, the main idea of LBO is to use a label algorithm to select and insert the best candidate BSSs into routes at high speed and high quality. First, the LBO removes all of the BSSs in each route and the order of customers will be fixed. In this case, the battery driving range constraints may be violated. Second, the LBO finds the possible insertion locations for each route and selects the BSSs with the minimum insertion costs to insert into the corresponding routes. This procedure will be stopped until all routes satisfy the battery driving range constraints. An overview of our LBO process is given in Algorithm 4, and the specific implementation details are described

Algorithm 4 Label-Based BSS Optimization Algorithm (LBO).

Require: A solution S_0 of the 2E-EVRP-BSS;

Ensure: An improved solution S^* of the 2E-EVRP-BSS;

```

1: Get the route set  $R$  from solution  $S$ ;
2: Create a route set  $R^* \leftarrow \emptyset$ ;
3: for  $r \in R$  do
4:   Create the current best route  $r^* \leftarrow r$ ;
5:   Remove all the stations of route  $r$ ;
6:   Create a route TreeSet  $TR \leftarrow \emptyset$ ;
7:    $TR \leftarrow TR \cup \{r\}$ ;
8:   Create a counter  $c = 0$ ;
9:   while  $TR \neq \emptyset$  and  $c < n_{max}$  do
10:     $r' \leftarrow \text{pollFirst}(TR)$ ;
11:    Calculate  $B_{min}$ ,  $v^*$  and  $L$  for  $r'$ ;
12:    if  $B_{min} < 0$  then
13:      for  $v \in L$  do
14:        copy a new route  $r'_v$  from  $r'$ ;
15:        insert the BSS with the minimum insertion cost in front of
16:         $v$  of  $r'_v$ ;
17:       $TR \leftarrow TR \cup \{r'_v\}$ ;
18:    end for
19:    else
20:       $c = c + 1$ ;
21:      if  $r' > r^*$  then
22:         $r^* \leftarrow r'$ ;
23:      end if
24:    end while
25:    $R^* \leftarrow R^* \cup \{r^*\}$ ;
26: end for
27: On the basis of  $R^*$ , create a solution  $S^*$ ;
28: Return  $S^*$ ;
```

in the following part.

We can get a route set R from a known solution S of the 2E-EVRP-BSS (line 1). For each route r in R , some nodes may be unreachable because of the removal of all the BSSs in it. We need to extend the route by reinserting the BSSs into the appropriate locations. For a large number of new extended routes, a comparison mechanism based on label (f, c, n_s, b, l) is helpful to choose the best candidate route for the next extension, where f represents the feasibility, c denotes the travel cost, n_s denotes the number of BSSs in the route, b is the amount of violated battery level and l is the location of the first node that violates the battery driving range constraints. If the route is feasible, $f = 1$; otherwise, $f = 0$. Label (f, c, n_s, b, l) is better than label (f', c', n'_s, b', l') for the next extension when $f \geq f'$, $c \leq c'$, $n_s \leq n'_s$ and $l \geq l'$. We use an automatic sorting collection called TreeSet in Java to collect the new extended routes and to sort the routes on the basis of their labels (line 6). In the search procedure of route r , r^* is defined to record the current best route and TR is the collection of routes that need to be

extended. For one candidate route r' in TR , we calculate the remaining battery power B_v for each node (line 11). v is unreachable when $B_v < 0$. B_{min} denotes the minimum value of the remaining battery power for all nodes. r' is feasible when $B_{min} \geq 0$. If $B_{min} < 0$, r' is unfeasible. Then, v^* is defined as the first unreachable node. We need to find suitable insertion positions of the BSSs in L , where L is denoted as the set of the candidate insertion positions before v^* (line 12–16). If route r' is feasible, r' is assigned to r^* when r' is better than r^* ($r' > r^*$) (line 18–23). This extension process continues until $TR = \emptyset$ or the number of iterations get n_{max} . Finally, a new route set R^* is created after optimizing all of the routes in R , and an improved solution S^* of the 2E-EVRP-BSS is generated.

5. Computational experiments

This section presents the results of the numerical experiments performed to evaluate the performance of our CG-ALNS algorithm. First, we used newly designed small instances that can be solved by CPLEX 12.6 to assess the quality of our CG-ALNS solution. Second, we conducted tests on larger instances to assess the performance of CG-ALNS in the 2E-EVRP-BSS. Third, we demonstrate the strong performance concerning solution quality and runtime of our CG-ALNS on available benchmark instances of the related problem, i.e. 2E-VRP. Finally, economic analysis was performed to assess the effect on the result and the emission reduction efficiency (ERE) of improving battery performance in the future.

Instances of the 2E-EVRP-BSS are generated as described in Section 5.1. In Section 5.2 we tune the values of the parameters using the instances of the 2E-EVRP-BSS and analyze the performance of each operator in CG-ALNS. Computational results of the 2E-EVRP-BSS and the 2E-VRP instances are showed in Section 5.3. The ERE and specific conclusions are given in Section 5.4.

5.1. Generation of 2E-EVRP-BSS benchmark instances

As the 2E-EVRP-BSS is the first model of this type, there are no available benchmark instances to evaluate the solution methods for this problem at present. Hence, we created small-sized instances of the 2E-EVRP-BSS named Set 1 that were based on the 2E-VRP instances in Perboli et al. (2011). Set 2 to Set 6 of the instances for the 2E-EVRP-BSS are created on the basis of the 2E-VRP instances used in Crainic, Perboli, Mancini, and Tadei (2010), Perboli et al. (2011), Hemmelmayr et al. (2012), and Baldacci et al. (2013). Breunig et al. gave a summary of the 2E-VRP instances in Breunig et al. (2016). We named the new generated instances of the 2E-EVRP-BSS after them.

In our 2E-EVRP-BSS, the instances we made consisted of the following data: number and locations of the BSSs, battery swapping cost, battery driving range and battery consumption rates of both types of EVs. Without loss of generality, the location of the BSSs was generated randomly and the number of BSSs was set to be 1/5 of the nodes in the network, like Schneider, Andreas and Goeke did in Schneider et al. (2014). The unit battery swapping fee was set to 2 for the first echelon and 1 for the second echelon. Let d_{max} denote the maximum Euclidean distance between any two points on the network. The battery driving ranges of the large EVs and the small EVs were defined in a simple way as in Schneider et al. (2014). We set $B^1 = \lceil 1.6d_{max} \rceil$ and $B^2 = \lceil 0.8d_{max} \rceil$, respectively. We set the EV consumption rate in both echelons to 1 per kilometre.

Table 2 provides a summary of the generated instances, including the number of instances (Inst.) in the set and subset with the number of customers (n_c), satellites (n_s), BSSs (n_b), EVs of the first-echelon (k^1), EVs of the second-echelon (k^2), EVs of satellite s of the second-echelon (k_s^1), travelling cost of each echelon (c_{ij}^1 and c_{ij}^2), battery swapping cost of both echelons (c_b^1 and c_b^2), battery consumption rate of both echelons (h^1 and h^2) and unit handling cost

Table 2
Characteristics of the 2E-EVRP-BSS instances.

Set	Inst.	n_C	n_S	n_B	k^1	k^2	k_s^2	c_{ij}^1	c_{ij}^2	c_b^1	c_b^2	h^1	h^2	h_s
1	66	7	2	5	3	4	–	1	1	2	1	1	1	0
1	66	12	2	5	3	4	–	1	1	2	1	1	1	0
2a	6	21	2	6	3	4	–	1	1	2	1	1	1	0
	6	32	2	6	3	4	–	1	1	2	1	1	1	0
2b	6	50	2	10	3	5	–	1	1	2	1	1	1	0
	3	50	4	10	4	5	–	1	1	2	1	1	1	0
2c	6	50	2	10	3	5	–	1	1	2	1	1	1	0
	3	50	4	10	4	5	–	1	1	2	1	1	1	0
3a	6	21	2	6	3	4	–	1	1	2	1	1	1	0
	6	32	2	6	3	4	–	1	1	2	1	1	1	0
3b	6	50	2	10	3	5	–	1	1	2	1	1	1	0
3c	6	50	2	10	3	5	–	1	1	2	1	1	1	0
4a	18	50	2	10	3	6	–	1	1	2	1	1	1	0
	18	50	3	10	3	6	–	1	1	2	1	1	1	0
	18	50	5	10	3	6	–	1	1	2	1	1	1	0
4b	18	50	2	10	3	6	4	1	1	2	1	1	1	0
	18	50	3	10	3	6	3	1	1	2	1	1	1	0
	18	50	5	10	3	6	2	1	1	2	1	1	1	0
5	6	100	5	20	5	[15,32]	–	1	1	2	1	1	1	0
	6	200	10	20	5	[17,35]	–	1	1	2	1	1	1	0
	6	200	10	20	5	[30,63]	–	1	1	2	1	1	1	0
6a	9	50	[4,6]	10	2	50	1	1	2	1	1	1	1	0
	9	75	[4,6]	15	3	75	1	1	2	1	1	1	1	0
	9	100	[4,6]	20	4	100	1	1	2	1	1	1	1	0
6b	9	50	[4,6]	10	2	50	1	1	2	1	1	1	1	≠0
	9	75	[4,6]	15	3	75	1	1	2	1	1	1	1	≠0
	9	100	[4,6]	20	4	100	1	1	2	1	1	1	1	≠0

Table 3
Notation and description of the parameters.

Parameter	Notation and description
τ	Cooling rate of SA of CG-ALNS
P_{init}	Initial temperature control parameter of SA
ζ	Cooling rate of SA of ALNS
μ_1, μ_2	Control Parameters of the number of removed customers
α	Parameter of BSS-customer route removal operator(BCRR)
η	Parameter of advanced greedy insertion operator(AGI)
θ	Reactor factor in adaptive selection of operators
σ_1	Score of a new best found solution
σ_2	Score of a new improving solution
σ_3	Score of an accepted deteriorating solution

of freight in the satellites (h_s). All of these instances were generated according to the procedures done in Prins, Prodhon, and Wolfier-Calvo (2004), Crainic et al. (2010), Perboli et al. (2011), and Hemmelmayr et al. (2012).

5.2. Parameter tuning and operator analyses

In line with the tuning method in the literature (Ribeiro & Laporte, 2012; Ropke & Pisinger, 2006b), we selected ten instances from Set 2 to Set 6 (two instances from each set) and performed 10 runs by considering up to seven values for each parameter. Set 1 was omitted here because the size of the instance was too small and provided less reference value. For each parameter value, we calculated the average percent deviation from the the best-found solutions. Then, the value that had the least average percent deviation was chosen to conduct the following calculation. The process was repeated until all the parameters had been tuned. The initial values of some parameters were set according to Hemmelmayr et al. (2012); the others were set according to several experiments. Table 3 summarizes the notations of the parameters, and Table 4 gives their considered values and corresponding deviations. The final values of the parameters are marked in bold.

The sensitivity analysis of the removal operators operators were conducted by keeping one of them used in the experiments but all

insertion operators are involved, like the authors did in Yang and Sun (2015). We conducted a similar analysis for the insertion operators. The results are showed in Tables A.1 and A.2 of the Appendix A.1. The BPRR, RCR, BCBP, SO, BBUR, BCRR, SR, BGI, BR2I, BR3I, AGI, AR2I and AR3I are selected for the following computational experiments. Table 5 provides further analysis about their contributions to diversifying the structure of the solutions and escaping local optima. The second column gives the average solution deviation without this operator under several computational experiments. The algorithm was conducted by excluding each of the corresponding operators while keeping the others. The BSS-customer route removal operator had the largest deviation, followed by the BSS proportion route removal and the random customer removal. In the third column of Table 5, we show the average number of times a new best solution was found by each operator. The random customer removal operator had the largest value of column 3, followed by the battery best use removal and the basic regret-3 insertion. From several experiments, the operators with smaller value in Table 5 helped in diversifying the structure of the solutions and escaping local optima. Therefore, we kept these operators in the following experiments.

5.3. Computational results

This subsection presents the results of the numerical experiments performed to demonstrate the applicability of our models and to evaluate the performance of our CG-ALNS heuristic.

5.3.1. Performance of CG-ALNS on small 2E-EVRP-BSS instances

We used the generated small 2E-EVRP-BSS test instances (Set 1) to analyse the performance of our CG-ALNS algorithm. In the first 14 instances of the test, we randomly selected five nodes among the customers as BSSs, and these nodes were no longer considered as customers. In the last five instances of the test, we randomly selected five nodes among the customers as both BSSs and customers. Therefore, according to the benchmark instance, Set 1 had two kinds of instances: the first one with 7 customers, 2 satellites and 5 BSSs; the other one with 12 customers, 2 satellites and 5

Table 4
Parameter tuning.

Parameter		Initial value	Values tested					
τ	Value	0.995	0.992	0.993	0.994	0.996	0.997	0.998
	dev%	0.51	0.37	0.49	0.44	0.53	0.41	0.43
P_{init}	Value	1.5	1.2	1.3	1.4	1.6	1.7	1.8
	dev%	0.62	0.58	0.73	0.68	0.85	0.69	0.77
ζ	Value	0.995	0.992	0.993	0.994	0.996	0.997	0.998
	dev%	0.53	0.48	0.43	0.58	0.52	0.61	0.61
μ_1	Value	0.1	0.04	0.08	0.06	0.12	0.16	0.2
	dev%	0.32	0.41	0.37	0.57	0.45	0.33	0.34
μ_2	Value	0.3	0.24	0.26	0.28	0.32	0.34	0.36
	dev%	0.36	0.22	0.28	0.34	0.4	0.39	0.44
α	Value	2	1	1.5	2.5	3	3.5	4
	dev%	0.55	0.43	0.47	0.32	0.38	0.64	0.43
η	Value	0.5	0.2	0.3	0.4	0.6	0.7	0.8
	dev%	0.42	0.56	0.44	0.4	0.41	0.37	0.51
θ	Value	0.7	0.3	0.4	0.5	0.6	0.8	0.9
	dev%	0.81	1.1	0.66	0.64	0.74	0.59	0.71
σ_1	Value	33	27	29	31	35	37	39
	dev%	0.93	0.72	0.84	0.77	0.62	0.88	0.82
σ_2	Value	21	15	17	19	23	25	27
	dev%	0.86	0.82	0.79	0.92	0.64	0.88	0.72
σ_3	Value	6	0	2	4	8	10	12
	dev%	0.59	0.61	0.74	0.67	0.52	0.65	0.58

Table 5
Analysis on the removal and insertion operators.

Operator	Solution degradation without this operator	Average number of new best solutions found by the operator
Random customer removal	0.05	15.23
Satellite removal	0.01	2.84
Satellite opening	0.04	1.8
BSS-customer route removal	0.1	1.33
BSS proportion route removal	0.07	3.93
BSS cost based removal	0.03	6.35
Battery best use removal	0.01	10.48
Basic greedy insertion	0.02	2.74
Basic regret-2 insertion	0.03	4.5
Basic regret-3 insertion	0.03	10.05
Advanced greedy insertion	0.03	2.45
Advanced regret-2 insertion	0.03	5.33
Advanced regret-3 insertion	0.04	9.2

BSSs. We solved the instances with CG-ALNS and compared the obtained results to the optimal or near-optimal solution found by the MIP solver of CPLEX 12.6 using the 2E-EVRP-BSS formulation presented in Section 3.

Table 6 gives the instance description and part of results of the test. The columns “ n_c ”, “ n_s ” and “ n_B ” present the number of customers, satellites and BSSs of each instance, respectively. The column “t(seconds)” denotes the computing time (in seconds) of CPLEX and CG-ALNS separately. The column “Best” and “Avg. 10” provides the best results obtained with CPLEX and the average result found in 10 runs by CG-ALNS. The best result of CPLEX was received either from the optimal solution or from the best upper bound (marked by an underscore) found within 7200 seconds. The percentage deviation between the total cost found by CPLEX and that by CG-ALNS is provided by %dev¹.

It can be observed from Table 6 that the average computation time of our CG-ALNS for 19 instances was 33.37 seconds, which is significantly faster than that of CPLEX, which was 2917.58 seconds. These clearly show the performance of our CG-ALNS algorithm in solving small-sized 2E-EVRP-BSS instances to optimality in only a few seconds. These results show that our CG-ALNS is capable of determining the highly efficient EV routes of the 2E-EVRP-BSS and is reasonable for application to larger instances.

5.3.2. Performance of CG-ALNS on larger 2E-EVRP-BSS instances

Tables 7–13 show the results of the computational experiments on the new larger 2E-EVRP-BSS instances of Set 2 to Set 6. These tables show the objective values of our CG-ALNS with stopping conditions of 200K iterations and 2000K iterations, $K = 1000$. In these tables, column 1 gives the name of each instance; column “Best” gives the results that were found in longer runtimes, we set the longer runtime of CG-ALNS iterations equal to 2200K; column “%dev²” shows the percentage deviation of the “CG-ALNS 200K” solution from that of “Best”; column “%dev³” shows the percentage deviation of the “CG-ALNS 2000K” solution from that of “Best”; column “T(seconds) 200K” and column “T*(seconds) 200K” give the total runtime and the time when the best solution in 200K iterations was found in seconds.

These tables show that we can obtain good results at moderate computing times. “%dev²” and “%dev³” increased with increasing data size, which indicates that longer runtimes and more iterations are needed for better solutions. For the largest data size of Set 5 with 100 and 200 customers, the average value of “%dev²” was 0.90 and the average value of “%dev³” was 0.17, which are acceptable at certain runtimes.

5.3.3. Performance of CG-ALNS on 2E-VRP instances

We can consider the classic 2E-VRP as the 2E-EVRP-BSS with a relaxation of the battery driving range constraints when the

Table 6

Comparison of results obtained with CPLEX and CG-ALNS on the small-sized 2E-EVRP-BSS instances.

Instance	Description			CPLEX		CG-ALNS		%dev ¹
	n_C	n_S	n_B	Best	t(seconds)	Avg. 10	t(seconds)	
E-n13-k4-1-c7	7	2	5	203	1785	203	13	0
E-n13-k4-2-c7	7	2	5	203	2715	203	19	0
E-n13-k4-10-c7	7	2	5	203	290	203	4.	0
E-n13-k4-12-c7	7	2	5	221	1963	221	22	0
E-n13-k4-15-c7	7	2	5	217	465	221	8	0
E-n13-k4-22-c7	7	2	5	257	4023	257	22	0
E-n13-k4-26-c7	7	2	5	257	2342	257	21	0
E-n13-k4-35-c7	7	2	5	271	2304	271	5	0
E-n13-k4-36-c7	7	2	5	271	1821	271	7	0
E-n13-k4-39-c7	7	2	5	214	1242	214	16	0
E-n13-k4-43-c7	7	2	5	214	156	214	13	0
E-n13-k4-48-c7	7	2	5	217	44	217	9	0
E-n13-k4-57-c7	7	2	5	257	43	257	11	0
E-n13-k4-62-c7	7	2	5	277	233	277	6	0
E-n13-k4-1-c12	12	2	5	<u>340</u>	7200	335	88	−1.49
E-n13-k4-2-c12	12	2	5	<u>361</u>	7200	350	93	−3.14
E-n13-k4-17-c12	12	2	5	<u>354</u>	7200	346	148	−2.31
E-n13-k4-32-c12	12	2	5	<u>363</u>	7200	342	31	−6.14
E-n13-k4-58-c12	12	2	5	<u>477</u>	7200	441	98	−8.16
Avg.	–	–	–	–	2917	–	33.37	−1.12

Table 7

Results and runtimes for Set 2 for the 2E-EVRP-BSS by CG-ALNS.

Instance	Best	CG-ALNS 200K	%dev ²	CG-ALNS 2000K	%dev ³	T(seconds)200K	T*(seconds)200K
Set2a							
E-n22-k4-s6-17	433.15	434.09	0.22	433.15	0.00	35	23
E-n22-k4-s8-14	395.58	396.47	0.22	395.58	0.00	28	19
E-n22-k4-s9-19	494.09	494.39	0.06	494.39	0.06	58	31
E-n22-k4-s10-14	371.50	371.50	0.00	371.50	0.00	43	30
E-n22-k4-s11-12	440.03	442.10	0.47	441.11	0.24	44	30
E-n22-k4-s12-16	401.90	401.90	0.00	401.90	0.00	79	52
E-n33-k4-s1-9	754.67	754.67	0.00	754.67	0.00	302	229
E-n33-k4-s2-13	745.38	745.38	0.00	745.38	0.00	463	303
E-n33-k4-s3-17	715.48	717.21	0.24	715.48	0.00	230	180
E-n33-k4-s4-5	802.22	807.62	0.67	805.31	0.38	243	176
E-n33-k4-s7-25	779.13	779.13	0.00	779.13	0.00	261	239
E-n33-k4-s14-22	795.31	800.12	0.60	797.68	0.30	199	172
Avg.	594.04	595.38	0.21	594.61	0.08	165.42	123.67
Set2b							
E-n51-k5-s2-17	597.49	602.12	0.77	597.49	0.00	99	53
E-n51-k5-s4-46	710.81	713.14	0.33	711.76	0.13	143	83
E-n51-k5-s6-12	583.04	587.49	0.76	585.83	0.48	201	179
E-n51-k5-s11-19	600.56	605.19	0.77	602.58	0.34	277	159
E-n51-k5-s27-47	583.54	583.54	0.00	583.54	0.00	59	31
E-n51-k5-s32-37	747.76	753.68	0.79	752.93	0.69	107	79
E-n51-k5-s2-4-17-46	600.18	602.55	0.39	600.18	0.00	249	178
E-n51-k5-s6-12-32-37	585.54	588.80	0.55	586.33	0.13	159	125
E-n51-k5-s11-19-27-47	539.14	540.74	0.30	540.38	0.23	247	201
Avg.	616.45	619.69	0.52	617.89	0.22	171.22	120.89
Set 2c							
E-n51-k5-s2-17	624.32	630.74	1.02	627.18	0.46	114	77
E-n51-k5-s4-46	764.22	764.22	0.00	764.22	0.00	96	58
E-n51-k5-s6-12	612.48	630.10	2.80	617.58	0.83	160	126
E-n51-k5-s11-19	684.31	701.26	2.42	688.74	0.64	305	266
E-n51-k5-s27-47	583.54	583.54	0.00	583.54	0.00	127	103
E-n51-k5-s32-37	814.63	822.76	0.99	814.63	0.00	224	185
E-n51-k5-s2-4-17-46	862.18	870.39	0.94	870.39	0.94	348	273
E-n51-k5-s6-12-32-37	626.45	650.83	3.75	626.45	0.00	236	192
E-n51-k5-s11-19-27-47	582.36	588.64	1.07	585.61	0.55	184	132
Avg.	683.83	693.61	1.44	686.48	0.38	199.33	156.89

Table 8
Results and runtimes for Set 3 for the 2E-EVRP-BSS by CG-ALNS.

Instance	Best	CG-ALNS 200K	%dev ²	CG-ALNS 2000K	%dev ³	T(seconds)200K	T*(seconds)200K
Set3a							
E-n22-k4-s13-14	532.79	532.79	0.00	532.79	0.00	124	82
E-n22-k4-s13-16	521.40	523.15	0.33	522.15	0.14	123	73
E-n22-k4-s13-17	496.38	498.43	0.41	498.06	0.34	62	49
E-n22-k4-s14-19	507.12	508.31	0.23	507.12	0.00	88	61
E-n22-k4-s17-19	512.80	513.76	0.19	512.80	0.00	72	59
E-n22-k4-s19-21	528.58	530.58	0.38	528.58	0.00	81	63
E-n33-k4-s16-22	748.58	751.53	0.39	748.58	0.00	57	48
E-n33-k4-s16-24	747.99	752.71	0.63	749.01	0.14	134	107
E-n33-k4-s19-26	680.36	685.01	0.68	682.52	0.32	331	261
E-n33-k4-s22-26	693.40	699.11	0.82	696.39	0.43	163	142
E-n33-k4-s24-28	684.98	689.49	0.65	686.77	0.26	108	76
E-n33-k4-s25-28	684.98	684.98	0.00	684.98	0.00	103	85
Avg.	611.61	614.15	0.39	612.48	0.14	120.50	92.17
Set3b							
E-n51-k5-s12-18	759.65	766.24	0.86	761.03	0.18	142	121
E-n51-k5-s12-41	732.98	741.23	1.11	737.51	0.61	245	174
E-n51-k5-s12-43	852.07	859.22	0.83	852.07	0.00	182	163
E-n51-k5-s39-41	899.35	903.04	0.41	899.36	0.00	214	163
E-n51-k5-s40-41	964.47	968.71	0.44	964.82	0.04	179	162
E-n51-k5-s40-43	915.26	924.30	0.98	918.06	0.30	205	183
Avg.	853.96	860.46	0.77	855.48	0.19	194.50	161.00
Set3c							
E-n51-k5-s13-19	679.59	702.72	3.29	684.27	0.68	217	183
E-n51-k5-s13-42	656.74	662.41	0.86	656.74	0.00	192	166
E-n51-k5-s13-44	710.76	722.81	1.67	722.81	1.67	314	268
E-n51-k5-s40-42	909.32	931.42	2.37	920.78	1.24	284	223
E-n51-k5-s41-42	970.52	1012.93	4.19	995.43	2.50	236	197
E-n51-k5-s41-44	925.63	987.85	6.30	964.93	4.07	265	214
Avg.	808.76	836.69	3.11	824.16	1.70	251.33	208.50

battery driving range is large enough and no BSSs are required. Tables 14–20 show the best solutions of the benchmark instance calculated by CG-ALNS. Columns “HCC Avg. 5” and “HCC (Best)” show the average results for five runs and the best solution found at longer runtimes given by Hemmelmayr et al. (2012), respectively, whose ALNS algorithm has been proven to have a good performance; columns “BSHV Avg. 5” and “BSHV (Best 5)” show the average results for five runs and the best solution found for these five runs given by Breunig et al. (2016), respectively, whose algorithm is known as the best performing heuristic so far; column “BKS” shows the best-known solution found in the literature, which is summarized in Breunig et al. (2016), and the solutions marked with asterisks were proven to be optimal; column “CG-ALNS (Avg. 5)” gives the average solution calculated by CG-ALNS for five runs; column “CG-ALNS (Best 5)” gives the best solutions found in these five runs; column “T(seconds)” and column “T*(seconds)” give the average overall runtime of CG-ALNS and the average time that the best solution was found in the five runs, respectively. Our solutions by CG-ALNS are marked in bold if they are equal to those of the BKS.

From Tables 14–20, for the instances with $n_c \leq 50$ (Set 2a and Set 3a), we obtained the same results as those of the BKS; for the instances of $n_c = 50$ (Set 2b, Set 2c, Set 3b, Set 3c Set 4a and Set 4b), our results obtained by CG-ALNS only had a slight deviation from those of the BKS. Our $T(\text{seconds})$ and $T^*(\text{seconds})$ were larger than the corresponding time in Hemmelmayr et al. (2012) and Breunig et al. (2016). This is because CG-ALNS is not specifically tailored to the classic 2E-VRP. When we use CG-ALNS to solve the classic 2E-VRP, the battery driving range is set large enough to avoid visiting BSSs. However, from the view of the execution of CG-ALNS, CG-ALNS still need to decide whether the battery driving ranges is violated in each iteration, and it is time consuming.

In summary, we can obtain good results of 2E-VRP with moderate computing time.

5.4. Economic analysis and specific conclusions

In this section, we analyse two parts: the first one is the sensitivity of the result to the battery driving range of EVs of each echelon, and the other is the ERE by using EVs instead of ICVs. To analyse the sensitivity of the result to the battery driving range, we changed the battery driving range of one echelon by fixing the battery driving range of the other echelon. CG-ALNS was performed five times for each instance, and the default parameter configuration and the best results were reported. Columns “ B^1 ” and “ B^2 ” give the variation percentage to the base value of the battery driving range in each echelon, respectively. Columns “ n_{b1} ” and “ n_{b2} ” give the number of BSSs visited in the result of the first echelon and the second echelon, respectively. Columns “ n_{k1} ” and “ n_{k2} ” give the number of routes in the result of the first echelon and the second echelon, respectively. Columns “ L^1 ” and “ L^2 ” give the length of the longest route in the result of the first echelon and the second echelon, respectively. Column “Obj.” gives the objective values of the instances. Columns 11–12 provide the result of the ERE of nitrogen oxides (NOx) and particulate emission. ERE is defined as $(\text{Best} - \text{BKS}) / (Er_x^1 * \text{BKS}^1 + Er_x^2 * \text{BKS}^2)$, which calculates the marginal cost of reducing the emission. BKS^1 and BKS^2 denote the first echelon part value and the second echelon part value of BKS, respectively. $(\text{Best} - \text{BKS})$ is the increased cost when adopting EVs instead of diesel vehicles, and $(Er_x^1 * \text{BKS}^1 + Er_x^2 * \text{BKS}^2)$ is the total emission of diesel vehicles in the best-known solutions. Based on the research by Zhang et al. (2016), the emission of gaseous and particulate pollutants exhaust are influenced by the speed,

Table 9

Results and runtimes for Set 4a for the 2E-EVRP-BSS by CG-ALNS.

Instance	Best	CG-ALNS 200K	%dev ²	CG-ALNS 2000K	%dev ³	T(seconds)200K	T*(seconds)200K
Instance50-1	1785.52	1799.57	0.78	1789.52	0.22	212	185
Instance50-2	1446.90	1453.57	0.46	1450.13	0.22	245	211
Instance50-3	1789.08	1798.83	0.54	1789.08	0.00	164	128
Instance50-4	1462.04	1469.14	0.48	1465.67	0.25	135	110
Instance50-5	2204.30	2213.53	0.42	2210.34	0.27	67	48
Instance50-6	1339.48	1350.92	0.85	1344.21	0.35	379	326
Instance50-7	1526.48	1538.35	0.77	1533.19	0.44	229	176
Instance50-8	1541.63	1546.27	0.30	1541.63	0.00	484	396
Instance50-9	1609.18	1614.32	0.32	1609.18	0.00	77	54
Instance50-10	1446.92	1470.04	1.57	1452.77	0.40	180	157
Instance50-11	2166.48	2185.13	0.85	2176.36	0.45	235	184
Instance50-12	1432.77	1445.35	0.87	1443.75	0.76	1003	914
Instance50-13	1560.52	1593.49	2.07	1572.34	0.75	114	82
Instance50-14	1531.81	1542.65	0.70	1535.89	0.27	189	145
Instance50-15	1710.4	1725.46	0.87	1710.40	0.00	143	86
Instance50-16	1416.28	1423.16	0.48	1416.28	0.00	127	91
Instance50-17	2354.27	2367.43	0.56	2358.99	0.20	148	124
Instance50-18	1232.61	1242.41	0.79	1234.92	0.19	133	105
Instance50-19	1868.48	1880.12	0.62	1874.42	0.32	940	883
Instance50-20	1348.74	1357.71	0.66	1356.47	0.57	587	485
Instance50-21	1591.01	1598.05	0.44	1594.59	0.22	525	479
Instance50-22	1347.45	1350.68	0.24	1347.45	0.00	842	695
Instance50-23	1816.34	1816.34	0.00	1816.34	0.00	1330	1064
Instance50-24	1500.66	1512.32	0.77	1504.76	0.27	206	176
Instance50-25	1705.64	1713.23	0.44	1705.64	0.00	344	282
Instance50-26	1270.85	1273.16	0.18	1270.85	0.00	726	683
Instance50-27	1752.40	1752.40	0.00	1752.40	0.00	482	410
Instance50-28	1259.63	1263.62	0.32	1260.65	0.08	1494	1187
Instance50-29	1814.92	1830.36	0.84	1814.92	0.00	472	430
Instance50-30	1239.07	1251.68	1.01	1244.86	0.47	639	564
Instance50-31	1562.14	1589.73	1.74	1586.11	1.51	1559	1371
Instance50-32	1244.64	1246.28	0.13	1244.64	0.00	685	589
Instance50-33	1706.62	1714.99	0.49	1712.49	0.34	1662	1217
Instance50-34	1240.30	1242.78	0.20	1240.30	0.00	347	258
Instance50-35	1770.54	1790.22	1.10	1784.46	0.78	1195	857
Instance50-36	1249.77	1250.23	0.04	1249.87	0.01	430	361
Instance50-37	1544.83	1546.82	0.13	1544.83	0.00	497	442
Instance50-38	1247.04	1261.71	1.16	1258.49	0.91	1549	1190
Instance50-39	1576.00	1579.00	0.19	1577.94	0.12	1317	922
Instance50-40	1246.92	1250.18	0.26	1246.92	0.00	452	406
Instance50-41	1697.44	1706.35	0.52	1703.62	0.36	1008	825
Instance50-42	1272.99	1276.12	0.25	1272.99	0.00	1534	1421
Instance50-43	1495.40	1505.68	0.68	1502.57	0.48	648	603
Instance50-44	1122.76	1124.70	0.17	1122.76	0.00	259	223
Instance50-45	1560.20	1570.15	0.63	1566.83	0.42	1604	1487
Instance50-46	1118.46	1127.17	0.77	1121.25	0.25	1480	1292
Instance50-47	1601.27	1603.49	0.14	1601.27	0.00	1635	1277
Instance50-48	1136.90	1148.45	1.01	1140.38	0.31	398	365
Instance50-49	1511.17	1516.17	0.33	1511.17	0.00	1541	1213
Instance50-50	1153.52	1160.30	0.58	1156.46	0.25	856	772
Instance50-51	1588.65	1590.78	0.13	1588.65	0.00	584	510
Instance50-52	1148.61	1152.37	0.33	1150.41	0.16	671	586
Instance50-53	1588.82	1593.12	0.27	1588.82	0.00	477	426
Instance50-54	1144.20	1153.88	0.84	1146.64	0.21	572	492
Avg.	1511.13	1520.00	0.58	1514.78	0.24	663.17	554.91

acceleration and engine load of vehicles. They calculated the average NOx emission rate and particulate emission rate of heavy duty diesel truck (Er_x^1) was 7.29 and 0.60 (grams/kilometers), respectively. The average NOx emission rate and particulate emission rate of light duty diesel truck (Er_x^2) was 5.53 and 0.14 (grams/kilometers), respectively. Based on the data, the ERE in Table 21 are obtained.

Based on the BSS, the 2E-EVRP-BSS aims to introduce the EVs into 2E-VRP and enrich the application of EVs in practice. Some constraints on the battery driving range are given special consider-

ation. Although the algorithm parameters and the computational instances affect the computational results, some specific conclusions are generalized as follows.

1) The battery driving range of EVs is an important factor to reduce the two-echelon distribution costs of logistics enterprises. From Table 21, if the battery driving range of the first echelon decreases by 10% of the base value, the objective value increases, whose increase rates are 2.1%, 1.8%, 0.1% and 1.1%. If the battery driving range of the first echelon increases by 10% of the base value, the objective value reduces, whose reduce rates are -0.8%,

Table 10

Results and runtimes for Set 4b for the 2E-EVRP-BSS by CG-ALNS.

Instance	Best	CG-ALNS 200K	%dev ²	CG-ALNS 2000K	%dev ³	T(seconds)200K	T*(seconds)200K
Instance50-1	1785.52	1799.57	0.78	1789.52	0.22	158	89
Instance50-2	1446.90	1453.57	0.46	1450.13	0.22	282	172
Instance50-3	1789.08	1798.83	0.54	1789.08	0.00	87	72
Instance50-4	1462.04	1469.14	0.48	1465.67	0.25	102	84
Instance50-5	2204.30	2213.53	0.42	2210.34	0.27	79	62
Instance50-6	1339.48	1350.92	0.85	1344.21	0.35	459	354
Instance50-7	1504.02	1514.75	0.71	1510.32	0.42	158	129
Instance50-8	1532.94	1544.83	0.77	1539.21	0.41	342	277
Instance50-9	1583.29	1607.97	1.53	1588.43	0.32	98	62
Instance50-10	1410.42	1423.71	0.93	1413.63	0.23	201	187
Instance50-11	2132.93	2146.97	0.65	2138.42	0.26	147	102
Instance50-12	1432.77	1445.35	0.87	1443.75	0.76	1189	812
Instance50-13	1553.71	1568.32	0.93	1556.83	0.20	86	44
Instance50-14	1531.81	1542.65	0.70	1535.89	0.27	108	91
Instance50-15	1671.15	1680.01	0.53	1675.28	0.25	86	74
Instance50-16	1410.42	1413.63	0.23	1410.57	0.01	174	153
Instance50-17	2354.27	2367.43	0.56	2358.99	0.20	81	51
Instance50-18	1232.61	1242.41	0.79	1234.92	0.19	103	84
Instance50-19	1852.76	1867.32	0.78	1859.80	0.38	1086	836
Instance50-20	1348.74	1357.71	0.66	1356.47	0.57	606	527
Instance50-21	1591.01	1598.05	0.44	1594.59	0.22	446	341
Instance50-22	1347.45	1350.68	0.24	1347.45	0.00	711	528
Instance50-23	1805.99	1808.41	0.13	1806.02	0.00	1188	863
Instance50-24	1456.87	1468.30	0.78	1460.92	0.28	159	105
Instance50-25	1674.23	1688.52	0.85	1679.44	0.31	257	178
Instance50-26	1270.85	1273.16	0.18	1270.85	0.00	584	495
Instance50-27	1732.86	1745.62	0.73	1739.01	0.35	620	572
Instance50-28	1259.63	1263.62	0.32	1260.65	0.08	1608	1264
Instance50-29	1778.61	1792.04	0.75	1784.76	0.34	511	396
Instance50-30	1239.07	1251.68	1.01	1244.86	0.47	518	445
Instance50-31	1538.11	1540.83	0.18	1538.11	0.00	1831	1422
Instance50-32	1244.64	1246.28	0.13	1244.64	0.00	542	357
Instance50-33	1701.88	1714.99	0.76	1708.95	0.41	1508	1038
Instance50-34	1240.30	1242.78	0.20	1240.30	0.00	214	179
Instance50-35	1598.66	1607.72	0.56	1599.18	0.03	1343	971
Instance50-36	1249.77	1250.23	0.04	1249.87	0.01	304	203
Instance50-37	1544.83	1546.82	0.13	1544.83	0.00	478	298
Instance50-38	1220.76	1221.99	0.10	1221.85	0.09	1364	1063
Instance50-39	1576.00	1579.00	0.19	1577.94	0.12	1429	1238
Instance50-40	1221.31	1222.86	0.13	1221.31	0.00	366	296
Instance50-41	1681.04	1699.85	1.11	1686.21	0.31	894	639
Instance50-42	1266.00	1272.48	0.51	1271.00	0.39	1090	821
Instance50-43	1489.03	1496.54	0.50	1493.38	0.29	791	534
Instance50-44	1117.42	1118.57	0.10	1117.42	0.00	365	257
Instance50-45	1552.81	1563.64	0.69	1559.92	0.46	1943	1346
Instance50-46	1115.58	1117.46	0.17	1115.58	0.00	1735	1392
Instance50-47	1588.48	1600.81	0.77	1588.54	0.00	1580	1112
Instance50-48	1134.57	1148.45	1.21	1137.85	0.29	531	414
Instance50-49	1511.17	1516.17	0.33	1511.17	0.00	1409	1041
Instance50-50	1150.26	1156.96	0.58	1154.96	0.41	665	492
Instance50-51	1584.37	1590.57	0.39	1587.01	0.17	366	221
Instance50-52	1147.17	1149.21	0.18	1147.61	0.04	478	341
Instance50-53	1554.58	1567.73	0.84	1556.06	0.10	460	338
Instance50-54	1144.82	1151.35	0.57	1144.99	0.01	408	372
Avg.	1498.32	1506.89	0.55	1501.46	0.20	635.70	478.41

−1.4%, −1.0% and −0.2%. If the battery driving range of the second echelon decreases by 10% of the base value, the objective value increases, whose increase rates are 0.7%, 0.9%, 3.2% and 1.3%. If the battery driving range of the second echelon increases by 10% of the base value, the objective value reduces, whose reduce rates are −6%, −0.8%, −1.2% and −0.3%.

For saving the cost of the two-echelon distribution system, when logistics enterprises try to introduce EVs to deliver goods, they need to give priority to EVs with larger battery driving range. Meanwhile, considering that different logistics enterprises have different service scope and volume, the configuration of vehicle

types especially the purchase cost of EVs and battery driving range should be well-balanced according to their business condition and demand network characteristics.

2) Logistics enterprises should focus on the number of needed BSSs to support current business. In our experiments, the location of the BSSs was generated randomly and the number of BSSs was set to be 1/5 of the nodes in the network, like Schneider, Andreas and Goeke did in Schneider et al. (2014). From Table 21, the number of visited BSSs shows little change when battery driving range varies. The battery driving range does not much affect the number of needed BSSs. The reason maybe be-

Table 11
Results and runtimes for Set 5 for the 2E-EVRP-BSS by CG-ALNS.

Instance	Best	CG-ALNS 200K	%dev ²	CG-ALNS 2000K	%dev ³	T(seconds)200K	T*(seconds)200K
100-5-1	1825.67	1846.01	1.10	1831.05	0.29	4931	4127
100-5-1b	1559.31	1599.25	2.50	1559.93	0.04	4482	3036
100-5-2	1478.62	1479.93	0.09	1478.62	0.00	3501	2964
100-5-2b	930.34	933.53	0.34	932.68	0.25	1323	1021
100-5-3	1183.31	1190.31	0.59	1184.55	0.10	3656	2847
100-5-3b	981.43	981.43	0.00	981.43	0.00	1032	823
100-10-1	1354.26	1374.22	1.45	1355.29	0.08	13902	9927
100-10-1b	1052.81	1060.72	0.75	1056.01	0.30	13729	9906
100-10-2	1095.28	1103.79	0.77	1103.79	0.77	14284	11220
100-10-2b	936.08	944.42	0.88	939.48	0.36	6283	5092
100-10-3	1272.10	1286.07	1.09	1272.10	0.00	17249	13257
100-10-3b	1002.85	1012.10	0.91	1005.10	0.22	8214	6972
200-10-1	1937.70	1950.11	0.64	1938.79	0.06	4255	3710
200-10-1b	1522.16	1541.86	1.28	1524.31	0.14	15876	13442
200-10-2	1786.55	1796.30	0.54	1788.21	0.09	20998	17620
200-10-2b	1228.48	1241.12	1.02	1228.48	0.00	30191	27546
200-10-3	2113.42	2130.23	0.79	2114.25	0.04	15297	10384
200-10-3b	1502.12	1523.35	1.39	1507.94	0.39	12076	9903
Avg.	1375.69	1388.60	0.90	1377.89	0.17	10626.61	8544.28

Table 12
Results and runtimes for Set 6a for the 2E-EVRP-BSS by CG-ALNS.

Instance	Best	CG-ALNS 200K	%dev ²	CG-ALNS 2000K	%dev ³	T(seconds)200K	T*(seconds)200K
A-n51-4	836.40	838.25	0.22	836.40	0.00	367	303
A-n51-5	781.22	784.54	0.42	781.22	0.00	429	385
A-n51-6	852.26	860.64	0.97	856.35	0.48	273	241
A-n76-4	1704.64	1718.47	0.80	1715.42	0.63	1249	1184
A-n76-5	1635.95	1649.20	0.80	1642.86	0.42	1887	1662
A-n76-6	1922.92	1938.77	0.82	1927.42	0.23	2238	1945
A-n101-4	2176.48	2190.78	0.65	2183.35	0.31	3951	3301
A-n101-5	2348.53	2378.90	1.28	2366.94	0.78	4272	3849
A-n101-6	2317.42	2355.27	1.61	2320.69	0.14	4406	4160
B-n51-4	710.84	736.62	3.50	715.35	0.63	384	349
B-n51-5	852.23	869.31	1.96	854.48	0.26	463	427
B-n51-6	742.30	753.08	1.43	749.37	0.94	459	410
B-n76-4	1837.93	1851.43	0.73	1841.24	0.18	2379	2158
B-n76-5	1661.81	1674.18	0.74	1667.04	0.31	1741	1505
B-n76-6	1568.40	1585.60	1.08	1574.01	0.36	2402	2180
B-n101-4	2053.28	2100.72	2.26	2061.51	0.40	4065	3819
B-n101-5	1886.74	1913.52	1.40	1894.38	0.40	5257	4934
B-n101-6	2142.34	2158.42	0.74	2150.85	0.40	5077	4826
C-n51-4	810.40	816.47	0.74	814.62	0.52	306	280
C-n51-5	881.94	885.39	0.39	883.05	0.13	394	362
C-n51-6	898.45	904.24	0.64	901.50	0.34	375	328
C-n76-4	1824.40	1830.23	0.32	1826.68	0.12	1891	1573
C-n76-5	1760.18	1766.48	0.36	1763.05	0.16	3048	2529
C-n76-6	1806.25	1813.42	0.40	1808.73	0.14	2152	1806
C-n101-4	2057.81	2082.47	1.18	2073.25	0.74	4593	4155
C-n101-5	1994.90	2110.72	5.49	2105.44	5.25	5022	4610
C-n101-6	2162.17	2190.95	1.31	2174.03	0.55	4850	4331
Avg.	1564.01	1583.63	1.19	1573.68	0.55	2367.78	2133.78

cause both types of EVs can share BSSs and a BSS can be visited more than one time by the same EV. So, if the BSSs could be located in a more suitable location, we believe the number of needed BSSs and operational cost may be reduced, but not much. And we will study this strategy in the future research.

3) Logistics enterprises need to evaluate the tradeoffs between reducing carbon emissions and the cost of using EVs. In order to control the carbon emission, the government mostly has three

policies when dealing with carbon emission, setting carbon cap, carbon taxes, the platform of cap-and-trade. If logistics enterprises use traditional vehicles, they may emit more pollution than using EVs, their carbon emissions may exceed the carbon cap. It will cost more on carbon taxes or buying carbon off-sets. However, if logistics enterprises use EVs, they need to pay the cost of EV detours, battery swapping costs, time cost (because of the detours and battery swapping) and more purchase cost instead of pollution cost. From Table 21, we provide the ERE to help logistics enterprises to

Table 13
Results and runtimes for Set 6b for the 2E-EVRP-BSS by CG-ALNS.

Instance	Best	CG-ALNS 200K	%dev ²	CG-ALNS 2000K	%dev ³	T(seconds)200K	T*(seconds)200K
A-n51-4	838.36	838.36	0.00	838.36	0.00	385	324
A-n51-5	876.29	876.29	0.00	876.29	0.00	287	241
A-n51-6	985.74	990.18	0.45	985.74	0.00	331	294
A-n76-4	1625.97	1655.62	1.79	1631.18	0.32	1082	935
A-n76-5	1803.49	1847.80	2.40	1803.49	0.00	2190	1857
A-n76-6	1910.42	1957.53	2.41	1924.84	0.75	1437	944
A-n101-4	2180.04	2275.94	4.21	2261.15	3.59	4228	3149
A-n101-5	1953.29	1991.42	1.91	1976.06	1.15	3842	3321
A-n101-6	2099.73	2147.40	2.22	2125.36	1.21	4511	3984
B-n51-4	708.35	726.14	2.45	712.60	0.60	462	410
B-n51-5	812.17	827.76	1.88	814.29	0.26	365	304
B-n51-6	928.61	950.22	2.27	932.72	0.44	507	437
B-n76-4	1248.90	1274.27	1.99	1253.89	0.40	1942	1677
B-n76-5	1497.04	1521.33	1.60	1502.84	0.39	2490	2152
B-n76-6	1569.41	1579.95	0.67	1573.52	0.26	2208	1866
B-n101-4	2111.58	2118.78	0.34	2114.26	0.13	3643	3159
B-n101-5	1977.67	1996.23	0.93	1982.47	0.24	5048	4741
B-n101-6	2013.63	2104.4	4.31	2081.05	3.24	4155	3763
C-n51-4	967.55	992.62	2.53	984.25	1.70	291	254
C-n51-5	1125.45	1150.42	2.17	1136.39	0.96	359	296
C-n51-6	1187.86	1214.65	2.21	1195.31	0.62	304	268
C-n76-4	1716.48	1731.14	0.85	1725.47	0.52	968	840
C-n76-5	2014.84	2087.52	3.48	2042.26	1.34	2551	2072
C-n76-6	1920.49	1968.72	2.45	1942.18	1.12	1751	1585
C-n101-4	2337.15	2426.34	3.68	2401.51	2.68	1489	1105
C-n101-5	2337.45	2354.27	0.71	2349.03	0.49	4624	4301
C-n101-6	2308.94	2350.62	1.77	2316.60	0.33	3747	3229
Avg.	1594.70	1628.00	1.91	1610.49	0.84	2044.33	1759.56

Table 14
Results and runtimes for Set 2 for the 2E-VRP by CG-ALNS.

Instance	BKS	HCC			BSHV			CG-ALNS			
		Avg. 5	T(seconds)	T*(seconds)	Avg. 5	T(seconds)	T*(seconds)	Avg. 5	Best5	T(seconds)	T*(seconds)
Set 2a											
E-n22-k4-s6-17	417.07*	417.07	37	0	417.07	60	1	417.07	417.07	27	19
E-n22-k4-s8-14	384.96*	384.96	34	0	384.96	60	1	384.96	384.96	27	20
E-n22-k4-s9-19	470.60*	470.60	35	0	470.60	60	1	470.60	470.60	47	33
E-n22-k4-s10-14	371.50*	371.50	37	0	371.50	60	2	371.50	371.50	25	18
E-n22-k4-s11-12	427.22*	427.22	31	0	427.22	60	2	427.29	427.22	31	24
E-n22-k4-s12-16	392.78*	392.78	36	0	392.78	60	1	392.78	392.78	66	45
E-n33-k4-s1-9	730.16*	730.16	74	0	730.16	60	1	730.16	730.16	159	108
E-n33-k4-s2-13	714.63*	714.63	64	0	714.63	60	1	714.63	714.63	102	76
E-n33-k4-s3-17	707.48*	707.48	58	0	707.48	60	1	707.48	707.48	186	141
E-n33-k4-s4-5	778.74*	778.74	77	0	778.74	60	1	778.74	778.74	237	152
E-n33-k4-s7-25	756.85*	756.85	53.00	3	756.85	60	1	756.85	756.85	205	177
E-n33-k4-s14-22	779.05*	779.05	85	0	779.05	60	1	779.31	779.05	184	121
Avg.	577.59	577.59	51.75	0.25	577.59	60	1	577.59	577.59	108	77.83
Set 2b											
E-n51-k5-s2-17	597.49*	597.49	100	7.	597.49	60	1	597.49	597.49	88	45
E-n51-k5-s4-46	530.76*	530.76	173	0	530.76	60	4	530.76	530.76	138	78
E-n51-k5-s6-12	554.81*	554.80	149	2	554.80	60	3	556.03	554.81	104	72
E-n51-k5-s11-19	581.64*	581.64	182	6	581.64	60	3	582.12	581.64	179	135
E-n51-k5-s27-47	538.22*	538.22	136	1	538.22	60	1	538.37	538.22	40	29
E-n51-k5-s32-37	552.28*	552.28	141	1	552.28	60	2	552.28	552.28	89	58
E-n51-k5-s2-4-17-46	530.76*	530.76	154	1	530.76	60	3	530.76	530.76	251	201
E-n51-k5-s6-12-32-37	531.92*	531.92	150	0	531.92	60	4	531.92	531.92	152	102
E-n51-k5-s11-19-27-47	527.63*	527.63	147	1	527.63	60	2	527.63	527.63	206	188
Avg.	549.50	549.50	148.00	2.11	549.50	60	2	549.71	549.50	138.56	100.89
Set 2c											
E-n51-k5-s11-19	617.42				617.42	60	3	620.16	619.81	215	176
E-n51-k5-s11-19-27-47	530.76				530.76	60	1	530.76	530.76	189	162
E-n51-k5-s2-17	601.39				601.39	60	3	605.62	605.62	96	71
E-n51-k5-s2-4-17-46	601.39				601.39	60	4	601.39	601.39	337	162
E-n51-k5-s27-47	530.76				530.76	60	3	532.86	530.76	59	37
E-n51-k5-s32-37	752.59				752.59	60	5	756.82	755.28	77	32
E-n51-k5-s4-46	702.33				702.33	60	4	702.33	702.33	155	83
E-n51-k5-s6-12	567.42				567.42	60	5	569.36	567.42	95	47
E-n51-k5-s6-12-32-37	567.42				567.42	60	6	567.42	567.42	151	99
Avg.	607.94				607.94	60	4	609.64	608.98	152.67	96.56

Table 15
Results and runtimes for Set 3 for the 2E-VRP by CG-ALNS.

Instance	BKS	HCC			BSHV			CG-ALNS			
		Avg. 5	T(seconds)	T*(seconds)	Avg. 5	T(seconds)	T*(seconds)	Avg. 5	Best5	T(seconds)	T*(seconds)
Set 3a											
E-n22-k4-s13-14	526.15*	526.15	43	0	526.15	60	2	526.15	526.15	103	81
E-n22-k4-s13-16	521.09*	521.09	44	0	521.09	60	2	521.09	521.09	107	79
E-n22-k4-s13-17	496.38*	496.38	49	0	496.38	60	1	496.38	496.38	56	33
E-n22-k4-s14-19	498.80*	498.80	43	0	498.80	60	1	498.80	498.80	75	54
E-n22-k4-s17-19	512.80*	512.81	26	0	512.80	60	4	512.81	512.81	89	49
E-n22-k4-s19-21	520.42*	520.42	34	0	520.42	60	2	520.42	520.42	68	44
E-n33-k4-s16-22	672.17*	672.17	76	3	672.17	60	4	672.17	672.17	58	39
E-n33-k4-s16-24	666.02*	666.02	77	0	666.02	60	1	666.02	666.02	115	83
E-n33-k4-s19-26	680.36*	680.36	84	0	680.36	60	1	680.36	680.36	200	162
E-n33-k4-s22-26	680.36*	680.37	77	0	680.36	60	1	680.37	680.37	121	87
E-n33-k4-s24-28	670.43*	670.43	88	0	670.43	60	2	670.43	670.43	88	51
E-n33-k4-s25-28	650.58*	650.58	63	0	650.58	60	1	650.58	650.58	86	53
Avg.	591.30	591.30	58.67	0	591.30	60	2	591.30	591.30	97.17	67.92
Set3b											
E-n51-k5-s12-18	690.59	690.59	147	4	690.59	60	8	690.59	690.59	116	82
E-n51-k5-s12-41	683.05	683.05	133	38	683.05	60	11	683.89	683.05	123	97
E-n51-k5-s12-43	710.41	710.41	217	1	710.41	60	5	710.41	710.41	177	135
E-n51-k5-s39-41	728.54	728.54	155	18	728.54	60	7	728.54	728.54	216	172
E-n51-k5-s40-41	723.75	723.75	154	17	723.75	60	5	723.75	723.75	177	159
E-n51-k5-s40-43	752.15	752.15	158	15	752.15	60	12	753.19	753.19	199	139
Avg.	714.75	714.75	160.67	16.00	714.75	60	8	715.06	714.92	119.54	87.73
Set3c											
E-n51-k5-s13-19	560.73				560.73	60	10	560.73	560.73	148	107
E-n51-k5-s13-42	564.45				564.45	60	3	564.45	564.45	87	62
E-n51-k5-s13-44	564.45				564.45	60	2	564.45	564.45	105	91
E-n51-k5-s40-42	746.31				746.31	60	5	747.37	746.31	193	149
E-n51-k5-s41-42	771.56				771.56	60	15	771.56	771.56	132	116
E-n51-k5-s41-44	802.91				802.91	60	16	804.23	804.23	99	52
Avg.	668.40				668.40	60	9	668.80	668.62	127.33	96.17

Table 16
Results and runtimes for Set 4a for the 2E-VRP by CG-ALNS.

Instance	BKS	BSHV				CG-ALNS			
		Avg. 5	Best 5	T(seconds)	T*(seconds)	Avg.5	Best 5	T(seconds)	T*(seconds)
Instance50-1	1569.42*	1569.42	1569.42	60	4	1569.42	1569.42	184	93
Instance50-2	1438.33*	1438.32	1438.32	60	16	1444.33	1444.33	139	116
Instance50-3	1570.43*	1570.43	1570.43	60	8	1570.43	1570.43	82	47
Instance50-4	1424.04*	1424.04	1424.04	60	7	1424.04	1424.04	136	114
Instance50-5	2193.52*	2193.52	2193.52	60	10	2199.11	2195.26	91	77
Instance50-6	1279.87*	1279.89	1279.89	60	0	1279.87	1279.87	152	131
Instance50-7	1458.63*	1458.60	1458.60	60	2	1503.72	1498.00	104	88
Instance50-8	1363.74*	1363.76	1363.76	60	29	1363.76	1363.76	160	137
Instance50-9	1450.27*	1450.25	1450.25	60	5	1450.27	1450.27	76	59
Instance50-10	1407.64*	1407.65	1407.65	60	6	1407.65	1407.65	147	118
Instance50-11	2047.46*	2052.21	2047.43	60	3	2054.42	2050.00	87	63
Instance50-12	1209.42*	1209.46	1209.46	60	8	1209.42	1209.42	142	125
Instance50-13	1481.83*	1481.80	1481.80	60	7	1527.16	1513.60	69	44
Instance50-14	1393.61*	1393.64	1393.64	60	1	1393.61	1393.61	125	119
Instance50-15	1489.94*	1489.92	1489.92	60	16	1497.34	1492.88	74	31
Instance50-16	1389.17*	1389.20	1389.20	60	2	1389.20	1389.20	192	104
Instance50-17	2088.49*	2088.48	2088.48	60	15	2088.49	2088.49	124	83
Instance50-18	1227.61*	1227.68	1227.68	60	1	1227.81	1227.73	115	82
Instance50-19	1564.66*	1564.66	1564.66	60	3	1564.66	1564.66	213	155
Instance50-20	1272.97*	1272.98	1272.98	60	25	1272.97	1272.97	217	158
Instance50-21	1577.82*	1577.82	1577.82	60	2	1577.82	1577.82	84	63
Instance50-22	1281.83*	1281.83	1281.83	60	3	1281.83	1281.82	164	118
Instance50-23	1807.35*	1807.35	1807.35	60	8	1807.35	1807.35	295	246
Instance50-24	1282.69*	1282.69	1282.69	60	0	1282.68	1282.68	144	108
Instance50-25	1522.42*	1522.40	1522.40	60	4	1551.40	1537.10	68	60
Instance50-26	1167.46*	1167.47	1167.47	60	1	1167.46	1167.46	152	107
Instance50-27	1481.57*	1481.56	1481.56	60	42	1483.48	1482.92	205	183
Instance50-28	1210.44*	1210.46	1210.46	60	3	1210.44	1210.44	177	129
Instance50-29	1722.04	1722.06	1722.00	60	31	1723.03	1722.00	394	287
Instance50-30	1211.59*	1211.63	1211.63	60	12	1212.40	1212.40	185	148
Instance50-31	1490.34	1490.32	1490.32	60	7	1490.34	1490.34	179	163
Instance50-32	1199.00*	1199.05	1199.05	60	24	1199.13	1199.00	143	112
Instance50-33	1508.30	1508.32	1508.32	60	14	1508.30	1508.30	186	149
Instance50-34	1233.92*	1233.96	1233.96	60	7	1233.92	1233.92	311	220
Instance50-35	1718.41	1718.42	1718.42	60	41	1718.42	1718.42	124	83

(continued on next page)

Table 16 (continued)

Instance	BKS	BSHV				CG-ALNS			
		Avg. 5	Best 5	T(seconds)	T*(seconds)	Avg.5	Best 5	T(seconds)	T*(seconds)
Instance50-36	1228.89*	1228.95	1228.95	60	0	1235.10	1231.72	172	105
Instance50-37	1528.73*	1528.73	1528.73	60	25	1528.73	1528.73	254	209
Instance50-38	1169.21*	1169.20	1169.20	60	15	1169.20	1169.20	247	213
Instance50-39	1520.92*	1520.92	1520.92	60	17	1520.95	1520.92	436	337
Instance50-40	1199.42*	1199.42	1199.42	60	2	1199.42	1199.42	291	215
Instance50-41	1667.96*	1667.96	1667.96	60	9	1667.96	1667.96	582	437
Instance50-42	1194.54*	1194.54	1194.54	60	19	1195.94	1195.28	360	254
Instance50-43	1439.67*	1439.67	1439.67	60	14	1442.82	1440.88	233	181
Instance50-44	1045.13*	1045.14	1045.14	60	24	1047.23	1045.74	192	163
Instance50-45	1450.96*	1451.48	1450.95	60	3	1457.48	1452.61	437	384
Instance50-46	1088.77*	1088.79	1088.79	60	2	1090.10	1088.79	293	241
Instance50-47	1587.29*	1587.29	1587.29	60	15	1597.29	1597.29	411	365
Instance50-48	1082.20*	1082.21	1082.21	60	23	1082.20	1082.20	385	297
Instance50-49	1434.88*	1434.88	1434.88	60	14	1438.62	1434.88	138	114
Instance50-50	1083.12*	1083.16	1083.16	60	23	1084.13	1083.77	227	176
Instance50-51	1398.05*	1398.03	1398.03	60	21	1402.18	1400.22	344	268
Instance50-52	1125.67*	1125.69	1125.69	60	6	1126.37	1125.93	275	220
Instance50-53	1567.77*	1567.79	1567.79	60	21	1567.79	1567.79	401	354
Instance50-54	1127.61*	1127.66	1127.66	60	15	1127.66	1127.66	304	258
Avg.	1419.94	1420.05	1419.95	60	12	1423.46	1422.20	212	165

Table 17

Results and runtimes for Set 4b for the 2E-VRP by CG-ALNS.

Instance	BKS	HCC				BSHV				CG-ALNS			
		Avg 5	Best	T(seconds)	T*(seconds)	Avg. 5	Best 5	T(seconds)	T*(seconds)	Avg.5	Best 5	T(seconds)	T*(seconds)
Instance50-1	1569.42*	1569.42	1569.42	235	6	1569.42	1569.42	60	15	1569.42	1569.42	131	84
Instance50-2	1438.33*	1441.02	1438.33	155	43	1438.32	1438.32	60	6	1444.33	1444.33	151	71
Instance50-3	1570.43*	1570.43	1570.43	183	3	1570.43	1570.43	60	7	1570.43	1570.43	74	50
Instance50-4	1424.04*	1424.04	1424.04	130	11	1424.04	1424.04	60	7	1424.04	1424.04	94	50
Instance50-5	2193.52*	2194.11	2194.11	614	63	2193.52	2193.52	60	18	2199.11	2195.26	83	53
Instance50-6	1279.87*	1279.87	1279.87	99	2	1279.89	1279.89	60	0	1279.87	1279.87	119	86
Instance50-7	1408.57*	1458.63	1458.63	169	6	1408.58	1408.58	60	17	1454.17	1446.00	125	72
Instance50-8	1360.32*	1360.32	1360.32	205	5	1360.32	1360.32	60	8	1360.77	1360.32	129	82
Instance50-9	1403.53*	1450.27	1450.27	204	46	1403.53	1403.53	60	11	1447.84	1409.00	84	62
Instance50-10	1360.56*	1360.56	1360.56	174	1	1360.54	1360.54	60	1	1360.56	1360.56	176	127
Instance50-11	2047.46*	2059.88	2059.88	648	101	2054.60	2047.43	60	2	2054.42	2050.00	109	73
Instance50-12	1209.42*	1209.42	1209.42	205	44	1209.46	1209.46	60	20	1209.42	1209.42	71	51
Instance50-13	1450.93*	1481.83	1481.83	220	25	1450.95	1450.94	60	10	1468.32	1459.94	54	34
Instance50-14	1393.61*	1393.61	1393.61	189	6	1393.64	1393.64	60	3	1393.61	1393.61	116	76
Instance50-15	1446.83*	1489.94	1489.94	173	9	1466.84	1466.84	60	2	1468.01	1466.83	86	55
Instance50-16	1387.83*	1387.83	1387.83	147	6	1387.85	1387.85	60	12	1388.46	1388.14	162	131
Instance50-17	2088.49*	2088.49	2088.49	625	165	2088.48	2088.48	60	13	2088.49	2088.49	87	59
Instance50-18	1227.61*	1227.61	1227.61	94	3	1227.68	1227.68	60	5	1227.81	1227.73	91	67
Instance50-19	1546.28*	1546.28	1546.28	171	25	1546.28	1546.28	60	34	1546.28	1546.28	150	117
Instance50-20	1272.97*	1272.97	1272.97	99	12	1272.98	1272.98	60	11	1272.97	1272.97	229	174
Instance50-21	1577.82*	1577.82	1577.82	155	61	1577.82	1577.82	60	16	1577.82	1577.82	91	52
Instance50-22	1281.83*	1281.83	1281.83	127	2	1281.83	1281.83	60	4	1281.83	1281.82	185	132
Instance50-23	1652.98*	1652.98	1652.98	175	5	1652.98	1652.98	60	4	1652.98	1652.98	241	197
Instance50-24	1282.68*	1282.68	1282.68	110	2	1282.69	1282.69	60	1	1282.68	1282.68	132	84
Instance50-25	1408.57*	1440.84	1440.68	154	53	1408.58	1408.58	60	20	1447.98	1440.50	95	59
Instance50-26	1167.46*	1167.46	1167.46	96	0	1167.47	1167.47	60	16	1167.46	1167.46	103	76
Instance50-27	1444.50*	1447.79	1444.50	163	12	1444.49	1444.49	60	20	1445.79	1445.57	154	109
Instance50-28	1210.44*	1210.44	1210.44	143	7	1210.46	1210.46	60	6	1210.44	1210.44	142	105
Instance50-29	1552.66*	1561.81	1559.82	178	102	1552.66	1552.66	60	39	1563.82	1552.66	487	320
Instance50-30	1211.59*	1211.59	1211.59	132	5	1211.63	1211.63	60	5	1212.40	1212.40	135	94
Instance50-31	1440.86*	1440.86	1440.86	144	37	1440.85	1440.85	60	15	1440.86	1440.86	115	76
Instance50-32	1199.00*	1199.00	1199.00	102	11	1199.05	1199.05	60	21	1199.13	1199.00	121	89
Instance50-33	1478.86*	1478.86	1478.86	159	16	1478.87	1478.87	60	15	1478.86	1478.86	165	139
Instance50-34	1233.92*	1233.92	1233.92	93	4	1233.96	1233.96	60	11	1233.92	1233.92	201	172
Instance50-35	1570.72*	1570.80	1570.72	182	116	1570.73	1570.73	60	10	1570.72	1570.72	131	99
Instance50-36	1228.89*	1228.89	1228.89	123	6	1228.95	1228.95	60	6	1235.10	1231.72	143	98
Instance50-37	1528.73	1528.81	1528.73	143	55	1528.73	1528.73	60	27	1528.73	1528.73	276	218
Instance50-38	1163.07*	1163.07	1163.07	88	15	1163.07	1163.07	60	17	1163.07	1163.07	222	190
Instance50-39	1520.92*	1520.92	1520.92	158	33	1520.92	1520.92	60	25	1520.95	1520.92	399	243
Instance50-40	1163.04*	1165.24	1163.04	84	20	1163.04	1163.04	60	5	1168.04	1168.04	357	208
Instance50-41	1652.98*	1652.98	1652.98	150	12	1652.98	1652.98	60	14	1652.98	1652.98	624	469
Instance50-42	1190.17*	1190.17	1190.17	95	31	1190.17	1190.17	60	9	1190.90	1190.49	324	167
Instance50-43	1406.11*	1408.95	1406.11	151	60	1407.09	1406.10	60	13	1414.11	1413.38	291	151
Instance50-44	1035.03*	1035.32	1035.03	109	30	1035.05	1035.05	60	42	1036.98	1036.25	278	181
Instance50-45	1401.87*	1406.43	1403.10	144	104	1401.87	1401.87	60	21	1413.19	1405.19	384	296

(continued on next page)

Table 17 (continued)

Instance	BKS	HCC				BSHV				CG-ALNS			
		Avg 5	Best	T(seconds)	T*(seconds)	Avg. 5	Best 5	T(seconds)	T*(seconds)	Avg.5	Best 5	T(seconds)	T*(seconds)
Instance50-46	1058.11*	1058.97	1058.11	74	17	1058.10	1058.10	60	16	1063.11	1058.29	345	255
Instance50-47	1552.66*	1564.41	1559.82	185	103	1552.66	1552.66	60	24	1558.48	1553.48	466	370
Instance50-48	1074.50*	1074.50	1074.50	83	2	1074.51	1074.51	60	4	1074.50	1074.50	237	104
Instance50-49	1434.88	1435.28	1434.88	140	81	1434.88	1434.88	60	9	1438.62	1434.88	152	101
Instance50-50	1065.25*	1065.25	1065.25	92	16	1065.30	1065.30	60	33	1065.25	1065.25	160	125
Instance50-51	1387.51*	1387.72	1387.51	138	46	1387.51	1387.51	60	19	1391.07	1388.06	322	203
Instance50-52	1103.42*	1103.76	1103.42	102	47	1103.47	1103.47	60	17	1104.31	1103.42	376	301
Instance50-53	1545.73*	1545.73	1545.73	148	37	1545.76	1545.76	60	21	1545.73	1545.73	320	287
Instance50-54	1113.62*	1113.62	1113.62	90	2	1113.66	1113.66	60	5	1113.17	1113.17	266	150
Avg.	1397.04	1401.39	1400.96	169.43	32.07	1397.21	1397.06	60.00	13.56	1401.36	1399.22	199	139

Table 18

Results and runtimes for Set 5 for the 2E-VRP by CG-ALNS.

Instance	BKS	HCC				BSHV				CG-ALNS			
		Avg. 5	Best	T(seconds)	T*(seconds)	Avg. 5	Best 5	T(seconds)	T*(seconds)	Avg. 5	Best 5	T(seconds)	T*(seconds)
100-5-1	1564.46*	1588.73	1565.45	353	116	1566.87	1564.46	900	201	1572.35	1570.97	1699	1302
100-5-1b	1108.62	1126.93	1111.34	397	45	1111.93	1108.62	900	176	1111.99	1108.65	2305	1981
100-5-2	1016.32*	1022.29	1016.32	406	117	1017.94	1016.32	900	75	1023.56	1017.33	2346	865
100-5-2b	782.25	789.05	782.25	340	170	783.07	782.25	900	152	794.44	782.67	1289	921
100-5-3	1045.29*	1046.67	1045.29	352	80	1045.29	1045.29	900	131	1046.67	1045.29	1796	1025
100-5-3b	828.54	828.99	828.99	391	127	828.54	828.54	900	62	834.30	834.21	1777	821
100-10-1	1124.93	1137.00	1130.23	429	136	1132.11	1124.93	900	567	1139.21	1127.04	10382	9912
100-10-1b	916.25	928.01	916.48	476	262	922.85	916.25	900	424	925.35	916.22	11142	9563
100-10-2	990.58	1009.49	990.58	356	232	1014.61	1002.15	900	471	1011.42	997.82	12056	10314
100-10-2b	786.61	773.58	768.61	432	157	786.64	774.11	900	416	769.26	768.61	5962	4392
100-10-3	1043.25	1055.28	1043.25	415	209	1053.55	1048.53	900	105	1056.22	1047.74	15746	10247
100-10-3b	850.92	861.88	850.92	418	29	858.72	854.90	900	175	866.10	851.36	6559	5923
200-10-1	1556.79	1626.83	1574.12	888	207	1598.46	1556.79	900	730	1586.43	1585.08	3177	2821
200-10-1b	1187.62	1239.79	1201.75	692	374	1217.23	1187.62	900	588	1221.25	1206.32	12943	9328
200-10-2	1365.74	1416.87	1374.74	1072	496	1406.16	1365.74	900	534	1407.88	1383.12	19832	15320
200-10-2b	1002.85	1018.57	1003.75	1058	221	1016.05	1002.85	900	721	1014.50	1002.84	28240	23318
200-10-3	1787.73	1808.24	1787.73	916	305	1809.44	1793.99	900	675	1811.99	1803.77	13021	10044
200-10-3b	1197.90	1208.38	1200.74	1217	478	1206.85	1197.90	900	523	1215.76	1209.02	10932	7361
Avg.	1118.81	1138.14	1121.81	589.33	208.94	1132.02	1120.62	900	373.7	1133.82	1125.45	8955.78	6969.89

Table 19

Results and runtimes for Set 6a for the 2E-VRP by CG-ALNS.

Instance	BKS	BSHV				CG-ALNS			
		Avg. 5	Best 5	T(seconds)	T*(seconds)	Avg.5	Best 5	T(seconds)	T*(seconds)
A-n51-4	652.00	652.00	652.00	60	19	652.00	652.00	214	181
A-n51-5	663.41	663.41	663.41	60	37	663.41	663.41	163	147
A-n51-6	662.51	662.51	662.51	60	23	674.28	674.28	185	156
A-n76-4	985.95	985.98	985.95	900	128	993.17	993.17	459	382
A-n76-5	979.15	981.19	979.15	900	286	982.64	979.15	373	322
A-n76-6	970.20	971.65	970.20	900	233	974.32	970.20	506	474
A-n101-4	1194.17	1194.38	1194.17	900	267	1221.61	1215.05	1267	1105
A-n101-5	1211.40	1215.89	1211.40	900	414	1231.38	1228.64	1526	1372
A-n101-6	1155.96	1161.91	1155.97	900	154	1174.23	1170.48	1352	1136
B-n51-4	563.98	563.98	563.98	60	6	567.84	567.84	217	184
B-n51-5	549.23	549.23	549.23	60	55	549.23	549.23	172	160
B-n51-6	556.32	556.32	556.32	60	39	556.32	556.32	249	213
B-n76-4	792.73	793.97	792.73	900	320	805.15	802.27	345	284
B-n76-5	784.19	784.27	784.19	900	190	790.81	788.49	273	249
B-n76-6	774.17	775.75	774.17	900	160	799.72	792.34	406	353
B-n101-4	939.21	939.79	939.21	900	377	1048.35	1044.91	1027	983
B-n101-5	969.13	971.27	969.13	900	161	989.49	985.74	1335	1146
B-n101-6	960.29	961.91	960.29	900	88	1290.4	1187.43	1293	1014
C-n51-4	689.18	689.18	689.18	60	13	689.18	689.18	228	194
C-n51-5	723.12	723.12	723.12	60	19	723.12	723.12	186	154
C-n51-6	697.00	697.00	697.00	60	46	697.00	697.00	272	249
C-n76-4	1054.89	1055.61	1054.89	900	339	1140.62	1132.47	436	370
C-n76-5	1115.32	1115.32	1115.32	900	113	1182.44	1176.61	517	489
C-n76-6	1060.52	1066.88	1060.52	900	474	1178.21	1173.35	450	428
C-n101-4	1302.16	1305.94	1302.16	900	236	1369.77	1364.43	1425	1362
C-n101-5	1305.82	1307.24	1305.82	900	141	1391.92	1382.40	1604	1341
C-n101-6	1284.48	1292.1	1284.48	900	446	1342.38	1337.62	1499	1247
Avg.	910.98	912.51	910.98	620	177	951.07	944.34	665.89	581.30

Table 20

Results and runtimes for Set 6b for the 2E-VRP by CG-ALNS.

Instance	BKS	BSHV				CG-ALNS			
		Avg. 5	Best 5	T(seconds)	T*(seconds)	Avg.5	Best 5	T(seconds)	T*(seconds)
A-n51-4	744.24	744.24	744.24	60	17	744.24	744.24	237	186
A-n51-5	811.52	811.51	811.51	60	49	811.51	811.51	301	266
A-n51-6	930.11	930.11	930.11	60	31	932.58	932.58	259	212
A-n76-4	1385.51	1385.51	1385.51	900	26	1395.39	1395.39	475	418
A-n76-5	1519.86	1519.86	1519.86	900	71	1519.86	1519.86	334	294
A-n76-6	1666.06	1666.28	1666.06	900	533	1671.44	1671.44	512	483
A-n101-4	1881.44	1884.48	1883.79	900	283	1930.20	1924.30	1173	962
A-n101-5	1709.06	1723.06	1711.95	900	318	1738.19	1734.86	1329	1184
A-n101-6	1777.69	1795.36	1791.44	900	100	1885.17	1880.63	1281	1094
B-n51-4	653.09	653.09	653.09	60	21	653.09	653.09	322	261
B-n51-5	672.10	672.10	672.10	60	51	677.65	677.65	278	262
B-n51-6	767.13	767.13	767.13	60	58	767.13	767.13	426	385
B-n76-4	1094.52	1094.52	1094.52	900	44	1094.52	1094.52	474	451
B-n76-5	1218.13	1218.12	1218.12	900	19	1224.74	1224.74	393	314
B-n76-6	1326.76	1328.90	1326.76	900	329	1333.05	1331.12	376	331
B-n101-4	1500.55	1500.80	1500.55	900	82	1520.58	1516.41	1441	1254
B-n101-5	1395.32	1398.05	1395.32	900	317	1417.25	1410.40	1273	1006
B-n101-6	1450.39	1455.05	1453.54	900	460	1478.75	1471.29	1214	1113
C-n51-4	866.58	866.58	866.58	60	22	866.58	866.58	268	232
C-n51-5	943.12	943.12	943.12	60	12	943.12	943.12	482	411
C-n51-6	1050.42	1050.42	1050.42	60	18	1066.71	1066.71	352	287
C-n76-4	1438.96	1439.39	1438.96	900	84	1441.22	1441.22	652	436
C-n76-5	1745.39	1745.49	1745.39	900	281	1750.29	1748.18	584	462
C-n76-6	1756.54	1759.40	1756.54	900	358	1761.62	1761.62	779	621
C-n101-4	2064.86	2076.36	2064.86	900	378	2081.68	2070.44	1489	1105
C-n101-5	1964.63	1974.39	1964.63	900	285	1983.36	1975.11	1266	965
C-n101-6	1861.50	1867.45	1861.50	900	401	1877.14	1872.42	1524	1018
Avg.	1340.57	1343.36	1341.39	620	172.1	1354.34	1352.09	722	593.07

Table 21

Sensitivity analysis of battery driving range and emission reduction efficiency (ERE).

Instance	B^1	B^2	n_{b1}	n_{b2}	n_{k1}	n_{k2}	L^1	L^2	Obj.	ERE	
										NOx	Particulate emission
E-n51-k5-s4-46	−10%	0%	3	4	3	6	65.12	128.86	728.49	0.0642	1.7605
	0%	−10%	2	4	2	5	119.42	118.13	719.10	0.0611	1.6769
	0%	0%	2	4	2	5	119.42	124.10	713.41	0.0593	1.6262
	10%	0%	2	4	2	5	119.42	146.38	707.59	0.0574	1.5744
	0%	10%	2	2	2	5	65.12	122.43	675.93	0.0471	1.2925
E-n51-k5-s6-12	−10%	0%	2	3	2	5	24.08	136.38	598.20	0.0137	0.4027
	0%	−10%	2	5	2	6	28.28	116.78	592.81	0.0120	0.3526
	0%	0%	2	3	2	5	24.08	124.54	587.49	0.0103	0.3033
	10%	0%	2	3	3	5	24.08	151.25	579.19	0.0077	0.2263
	0%	10%	2	2	3	5	28.28	117.46	582.42	0.0087	0.2563
E-n51-k5-s6-12-32-37	−10%	0%	2	3	2	5	24.08	136.38	589.58	0.0192	0.6315
	0%	−10%	2	4	3	5	59.67	117.31	607.60	0.0252	0.8287
	0%	0%	2	3	2	5	24.08	151.25	588.80	0.0189	0.6229
	10%	0%	1	3	3	5	28.28	117.46	582.42	0.0168	0.5530
	0%	10%	2	3	2	5	24.08	120.87	581.64	0.0165	0.5444
E-n51-k5-s11-19-27-47	−10%	0%	2	3	3	5	29.53	109.56	547.11	0.0065	0.2177
	0%	−10%	2	4	3	5	29.53	109.33	548.16	0.0069	0.2295
	0%	0%	2	3	3	5	29.53	119.98	540.74	0.0044	0.1465
	10%	0%	0	3	2	5	4.47	119.98	539.34	0.0039	0.1309
	0%	10%	2	3	3	5	29.53	119.98	539.14	0.0039	0.1287

compare the cost between using EVs and using traditional vehicles. In addition, Table 21 show that the value of ERE decreases with increasing battery driving range of both echelons. Therefore, logistics enterprises could evaluate their green vehicles plan for two echelon city logistics according to this indicator ERE obtained from our problem.

6. Conclusion and future work

In this paper, we presented the 2E-EVRP-BSS that considers the limited battery driving ranges and the battery swapping strategy at available BSSs. Furthermore, vehicle capacity constraints were also incorporated into the 2E-EVRP-BSS model to represent real-world

requirements. We developed a hybrid CG-ALNS heuristic that uses the strong accuracy effect of CG and involves an ALNS heuristic to efficiently search a large neighborhood. To assess the performance of the proposed solution approach, we conducted experiments on the basis of the benchmark instances of the literature. We demonstrated the strong performance of our algorithm by computational experiments on newly designed 2E-EVRP-BSS instances. The quality of our method was further substantiated by very convincing results on test instances of the related problem of the 2E-VRP. Finally, in the economic analysis, we performed several experiments to highlight the managerial implications of the interplay between battery driving ranges and the efficiency of vehicle emission reduction.

Our manuscript did not consider all realistic situations in the problem. Future work should extend the 2E-EVRP-BSS model by considering the battery recharging time and customer service time window. The capacity limitation of satellites and BSSs should be incorporated also into the 2E-EVRP-BSS.

Acknowledgments

The authors were supported by the [National Natural Science Foundation of China](#) (No. 71672065 and No. 71320107001), the Fundamental Research Funds for the Central Universities and The Wuhan Yellow Crane Talents Project. This work was completed while the last author (Huang) was at Clemson University. He is sincerely grateful to Clemson University for the resources provided to

complete this study. In addition, we thank Cheng Pei from Alibaba Cloud for his valuable guidance and advice on algorithm implementation and experimental analysis.

Appendix A.1

In the two tables, “Call” presents the number of times an operator has been used, “Weight” presents the average value of the final weight of each operator, the column “Filename” presents the names of the corresponding instances, and column “Avg.” denotes the average value of each instance. The results better than the average value are marked in bold, and was selected for the following computational experiments.

Table A.1
Sensitivity analysis of the removal operators.

Param.	Filename	BPRR	RCR	ReCR	BCBR	SO	SS	BBUR	BCRR	RRR	SR	Avg.
Call	E-n22-k4-s10-14	20018	19963	20052	20038	20062	20081	18878	20111	19703	21094	20000
	E-n22-k4-s11-12	20037	20112	19718	20137	19974	19964	20021	20036	19918	20083	20000
	E-n22-k4-s12-16	20050	20104	19786	20204	20028	19840	21025	20087	18849	20027	20000
	E-n22-k4-s6-17	20140	20259	20067	20130	20082	20013	20007	20067	19205	20030	20000
	E-n22-k4-s8-14	20027	20126	20061	20039	18971	20056	19970	21021	19714	20015	20000
	E-n22-k4-s9-19	20054	20149	19852	20231	21009	18870	20140	20047	19560	20088	20000
	E-n33-k4-s1-9	20271	21112	18794	20222	20016	19814	20088	20163	19677	19843	20000
	E-n33-k4-s14-22	20273	20262	19476	20241	20125	19592	20085	20090	19551	20305	20000
	E-n33-k4-s2-13	20168	20189	19924	20185	20014	19892	20061	20106	19275	20186	20000
	E-n33-k4-s3-17	21283	20161	19831	20262	20019	18610	20049	20019	19630	20136	20000
	E-n33-k4-s4-5	20150	20172	19795	20297	19992	19941	19927	20140	19516	20070	20000
	E-n33-k4-s7-25	20189	20130	19697	20255	20234	19706	19887	20091	19524	20287	20000
	E-n51-k5-s11-19-27-47	20081	20094	19859	19995	20084	19769	20131	20301	19698	19988	20000
	E-n51-k5-s11-19	20342	20289	19476	21362	20058	18463	20102	20133	19636	20139	20000
	E-n51-k5-s2-1	20094	20114	19622	20160	20050	19681	20204	20164	19929	19982	20000
	E-n51-k5-s2-4-17-46	21184	20070	19743	20264	20020	18731	20043	20148	19703	20094	20000
	E-n51-k5-s27-47	20329	20274	19434	20316	20146	19431	20096	20339	18533	21102	20000
	E-n51-k5-s32-37	20409	20131	19316	20345	21185	19273	20193	20229	18537	20382	20000
	E-n51-k5-s4-46	20437	21159	18578	20171	20038	19626	20039	20162	19647	20143	20000
	E-n51-k5-s6-12-32-37	20219	20099	19860	20202	20155	19527	20103	20139	19826	19870	20000
	E-n51-k5-s6-12	20179	20036	19576	20239	20053	19525	20096	20116	20050	20130	20000
Weight	E-n22-k4-s10-14	11.53	10.72	13.08	11.14	11.19	13.06	11.31	10.15	8.09	11.40	11.17
	E-n22-k4-s11-12	11.14	12.13	9.56	12.27	9.86	9.70	10.79	13.78	11.79	10.97	11.20
	E-n22-k4-s12-16	11.15	11.83	7.79	11.93	11.30	6.95	10.14	10.87	6.07	10.43	9.85
	E-n22-k4-s6-17	11.56	11.75	10.20	10.64	11.64	9.10	9.05	11.92	0.00	10.34	9.62
	E-n22-k4-s8-14	10.48	12.12	10.66	11.54	10.96	9.40	10.95	11.33	7.85	10.89	10.62
	E-n22-k4-s9-19	11.18	12.01	8.71	13.59	11.43	9.99	11.51	12.79	5.56	11.35	10.81
	E-n33-k4-s1-9	12.69	11.95	8.82	13.67	10.60	7.71	12.46	11.59	3.18	10.85	10.35
	E-n33-k4-s14-22	14.43	12.32	3.37	12.98	11.66	7.99	11.62	13.97	6.87	13.11	10.83
	E-n33-k4-s2-13	12.74	12.84	7.76	12.21	11.19	5.51	9.98	14.02	0.00	12.33	9.86
	E-n33-k4-s3-17	13.47	12.24	6.50	14.12	12.03	9.37	7.95	12.15	5.47	11.24	10.45
	E-n33-k4-s4-5	12.59	13.66	6.88	13.55	11.83	10.44	10.93	14.09	2.28	13.14	10.94
	E-n33-k4-s7-25	10.64	9.48	9.18	12.17	11.31	4.61	7.44	11.77	1.17	11.76	8.95
	E-n51-k5-s11-19-27-47	14.09	12.01	8.43	14.84	12.11	6.55	12.46	16.08	8.23	12.04	11.68
	E-n51-k5-s11-19	15.02	12.98	3.99	14.89	13.03	2.11	13.01	12.92	3.91	14.49	10.64
	E-n51-k5-s2-17	14.83	13.21	2.20	14.09	11.25	5.39	15.23	15.23	8.19	12.45	11.21
	E-n51-k5-s2-4-17-46	15.91	12.79	9.18	15.72	11.43	7.38	13.74	12.87	7.77	14.20	12.10
	E-n51-k5-s27-47	14.12	12.43	3.99	14.41	11.93	2.34	12.50	12.88	2.93	12.36	9.99
	E-n51-k5-s32-37	14.07	10.87	0.00	13.92	11.73	0.00	11.92	12.69	3.80	13.23	9.22
	E-n51-k5-s4-46	16.69	14.56	3.48	13.49	11.12	6.72	13.95	13.31	4.33	11.91	10.96
	E-n51-k5-s6-12-32-37	16.60	13.29	9.22	15.38	13.28	5.69	15.26	13.75	6.22	12.05	12.07
	E-n51-k5-s6-12s	14.03	11.72	4.12	14.86	13.01	4.62	14.69	13.05	11.24	14.00	11.53

Table A.2
Sensitivity analysis of the insertion operators.

Param.	Filename	BGI	BR2I	BR3I	BR4I	AGI	AR2I	AR3I	AR4I	Avg.
Call	E-n22-k4-s10-14	24241	25470	25102	24407	25026	25809	25108	24837	25000.00
	E-n22-k4-s11-12	26117	25119	23902	24955	24928	25212	24917	24850	25000.00
	E-n22-k4-s12-16	25038	25103	25113	24874	24988	25039	25019	24826	25000.00
	E-n22-k4-s6-17	25106	25040	26001	23625	25137	25243	25073	24775	25000.00
	E-n22-k4-s8-14	25109	25048	25048	24087	25813	25026	25050	24819	25000.00
	E-n22-k4-s9-19	25090	25036	25031	25022	23993	25043	26022	24763	25000.00
	E-n33-k4-s1-9	25038	24946	25019	24698	25109	25215	24936	25039	25000.00
	E-n33-k4-s14-22	24972	25198	25189	24721	25139	25079	25023	24679	25000.00
	E-n33-k4-s2-13	25012	25123	25132	24811	25021	25226	25088	24587	25000.00
	E-n33-k4-s3-17	25243	25113	25178	24765	25014	25020	25066	24601	25000.00
	E-n33-k4-s4-5	24194	25919	25189	24639	25117	25023	25198	24721	25000.00
	E-n33-k4-s7-25	25028	25107	24740	25067	25152	25081	25064	24761	25000.00
	E-n51-k5-s11-19-27-47	25289	25063	25144	24589	25003	25109	25191	24612	25000.00
	E-n51-k5-s11-19	25002	25009	25029	24904	25055	25019	26011	23971	25000.00
	E-n51-k5-s2-17	25099	25042	25010	24821	25147	25006	24809	25066	25000.00
	E-n51-k5-s2-4-17-46	25107	25098	25076	23822	25097	26005	25050	24745	25000.00
	E-n51-k5-s27-47	25010	25100	25004	26021	25051	25015	25050	23749	25000.00
	E-n51-k5-s32-37	26096	25156	25050	24924	25047	25077	25027	23623	25000.00
	E-n51-k5-s4-46	25016	25004	25821	25008	25019	25063	25064	24005	25000.00
	E-n51-k5-s6-12-32-37	25193	24972	24884	24847	25065	25021	25295	24723	25000.00
	E-n51-k5-s6-12	24824	26066	25053	24845	24925	23908	25354	25025	25000.00
Weight	E-n22-k4-s10-14	10.12	12.25	10.59	10.11	12.63	12.77	12.12	7.23	10.98
	E-n22-k4-s11-12	11.05	12.08	9.11	8.92	9.52	11.55	9.61	9.23	10.13
	E-n22-k4-s12-16	11.72	11.31	12.13	10.37	10.33	12.35	11.45	5.82	10.69
	E-n22-k4-s6-17	12.65	11.59	11.86	6.21	10.62	13.24	9.08	7.66	10.36
	E-n22-k4-s8-14	9.56	11.85	10.71	8.24	8.79	11.90	10.34	9.32	10.09
	E-n22-k4-s9-19	10.86	11.23	9.63	10.42	11.84	10.93	10.81	9.23	10.62
	E-n33-k4-s1-9	9.67	11.64	11.07	9.83	10.98	12.27	10.34	11.61	10.93
	E-n33-k4-s14-22	11.37	13.34	12.08	8.79	10.64	12.71	13.23	10.83	11.62
	E-n33-k4-s2-13	9.89	13.51	9.92	8.02	8.87	13.36	10.28	7.86	10.21
	E-n33-k4-s3-17	11.58	12.33	11.98	8.22	11.84	13.12	11.91	11.29	11.53
	E-n33-k4-s4-5	10.87	14.02	13.41	6.85	11.59	10.84	11.07	6.76	10.68
	E-n33-k4-s7-25	10.61	11.03	10.31	10.93	8.99	10.34	9.28	8.58	10.01
	E-n51-k5-s11-19-27-47	8.46	12.26	13.65	7.97	11.47	11.50	13.59	9.34	11.03
	E-n51-k5-s11-19	11.98	13.22	11.63	10.49	11.96	11.22	13.07	8.36	11.49
	E-n51-k5-s2-17	12.03	13.15	12.59	9.37	13.28	14.54	12.54	9.74	12.16
	E-n51-k5-s2-4-17-46	10.93	12.45	12.48	8.68	9.81	13.11	13.39	6.47	10.92
	E-n51-k5-s27-47	11.85	12.37	12.29	11.37	12.41	11.56	13.32	6.51	11.46
	E-n51-k5-s32-37	11.36	12.89	12.48	9.48	11.13	11.87	12.88	8.63	11.34
	E-n51-k5-s4-46	10.24	12.73	12.53	8.86	12.32	12.02	11.56	11.76	11.50
	E-n51-k5-s6-12-32-37	9.21	12.28	12.49	10.84	11.86	13.72	12.97	6.53	11.24
	E-n51-k5-s6-12	12.63	13.06	13.19	7.86	13.71	13.56	13.76	12.97	12.59

References

- Adler, J. D., & Mirchandani, P. B. (2014). Online routing and battery reservations for electric vehicles with swappable batteries. *Transportation Research Part B: Methodological*, 70, 285–302.
- Anderluh, A., Hemmelmayr, V. C., & Nolz, P. C. (2017). Synchronizing vans and cargo bikes in a city distribution network. *Central European Journal of Operations Research*, 25(2), 1–32.
- Archetti, C., Bianchessi, N., & Speranza, M. G. (2011). A column generation approach for the split delivery vehicle routing problem. *Networks*, 58(4), 241–254.
- Baldacci, R., Mingozzi, A., Roberti, R., & Calvo, R. W. (2013). An exact algorithm for the two-echelon capacitated vehicle routing problem. *Operations Research*, 61(2), 298–314.
- Breunig, U., Schmid, V., Hartl, R. F., & Vidal, T. (2016). A large neighbourhood based heuristic for two-echelon routing problems. *Computers & Operations Research*, 76, 208–225.
- Caramia, M., & Guerriero, F. (2010). A heuristic approach for the truck and trailer routing problem. *Journal of the Operational Research Society*, 61(7), 1168–1180.
- Christofides, N., & Eilon, S. (1969). An algorithm for the vehicle-dispatching problem. *Journal of the Operational Research Society*, 20(3), 309–318.
- Clarke, G. u., & Wright, J. W. (1964). Scheduling of vehicles from a central depot to a number of delivery points. *Operations Research*, 12(4), 568–581.
- Contardo, C., Hemmelmayr, V., & Crainic, T. G. (2012). Lower and upper bounds for the two-echelon capacitated location-routing problem. *Computers & Operations Research*, 39(12), 3185–3199.
- Crainic, T. G., Mancini, S., Perboli, G., & Tadei, R. (2008). Clustering-based heuristics for the two-echelon vehicle routing problem. CIRRELT, Montréal, CIRRELT-2008-46. <http://www.cirrelt.ca/DocumentsTravail/CIRRELT-2008-46.pdf>.
- Crainic, T. G., Mancini, S., Perboli, G., & Tadei, R. (2011). Multi-start heuristics for the two-echelon vehicle routing problem. In *European conference on evolutionary computation in combinatorial optimization* (pp. 179–190).
- Crainic, T. G., Mancini, S., Perboli, G., & Tadei, R. (2013). GRASP with path relinking for the two-echelon vehicle routing problem. In *Advances in metaheuristics* (pp. 113–125). Springer.
- Crainic, T. G., Perboli, G., Mancini, S., & Tadei, R. (2010). Two-echelon vehicle routing problem: a satellite location analysis. *Procedia-Social and Behavioral Sciences*, 2(3), 5944–5955.
- Crainic, T. G., Ricciardi, N., & Storch, G. (2009). Models for evaluating and planning city logistics systems. *Transportation Science*, 43(4), 432–454.
- Cuda, R., Guastaroba, G., & Speranza, M. (2015). A survey on two-echelon routing problems. *Computers & Operations Research*, 55, 185–199.
- Dantzig, G. B., & Wolfe, P. (1960). Decomposition principle for linear programs. *Operations Research*, 8(1), 101–111.
- Dellaert, N., Crainic, T., Van Woensel, T., & Saridarq, F. D. (2016). *Branch & price based algorithms for the two-echelon vehicle routing problem with time windows*. CIRRELT, Centre interuniversitaire de recherche sur les réseaux d'entreprise, la logistique et le transport= Interuniversity Research Centre on Enterprise Networks, Logistics and Transportation.
- Derigs, U., Pullmann, M., & Vogel, U. (2013). Truck and trailer routing-problems, heuristics and computational experience. *Computers & Operations Research*, 40(2), 536–546.
- Desaulniers, G. (2010). Branch-and-price-and-cut for the split-delivery vehicle routing problem with time windows. *Operations Research*, 58(1), 179–192.
- Desaulniers, G., Desrosiers, J., & Solomon, M. M. (2006). *Column generation*: Vol. 5. Springer Science & Business Media.
- Desaulniers, G., Erice, F., Irnich, S., & Schneider, M. (2016). Exact algorithms for electric vehicle-routing problems with time windows. *Operations Research*, 64(6), 1388–1405.
- Desrochers, M. (1988). An algorithm for the shortest path problem with resource constraints. In *Proceedings of the IEEE conference on computer vision and pattern recognition (CVPR)* (pp. 3454–3461).
- Desrochers, M., & Soumis, F. (1998). A generalized permanent labeling algorithm for the shortest path problem with time windows. *INFOR Information Systems and Operational Research*, 26(3), 191–212.

- Drexl, M. (2013). Applications of the vehicle routing problem with trailers and transshipments. *European Journal of Operational Research*, 227(2), 275–283.
- Dror, M., & Trudeau, P. (1989). Savings by split delivery routing. *Transportation Science*, 141–145.
- Dror, M., & Trudeau, P. (1990). Split delivery routing. *Naval Research Logistics (NRL)*, 37(3), 383–402.
- FedEx (2010). FedEx introduces first all-electric trucks to be used in the U.S. parcel delivery business. <http://about.van.fedex.com/newsroom/global-english/fedex-introduces-first-all-electric-trucks-to-be-used-in-the-u-s-parcel-delivery-business/>.
- Feillet, D., Dejax, P., Gendreau, M., & Gueguen, C. (2010). An exact algorithm for the elementary shortest path problem with resource constraints: Application to some vehicle routing problems. *Networks*, 44(3), 216–229.
- FREVUE (2016). Freight electric vehicles in urban Europe. <https://frevue.eu/>.
- Gillet, B. E., & Miller, L. R. (1974). A heuristic algorithm for the vehicle-dispatch problem. *Operations Research*, 22(2), 340–349.
- Golson, J. (2014). FedEx's new electric trucks get a boost from diesel turbines. <http://www.wired.com/2014/09/fedex-wrightspeed-diesel-ev-trucks/>.
- Gonzalez-Feliu, J. (2012). Cost optimisation in freight distribution with cross-docking: N-echelon location routing problem. *PROMET-Traffic&Transportation*, 24(2), 143–149.
- Gonzalezfeliu, J. (2011). Two-echelon transportation optimisation: A meta-narrative analysis. *Wpwm Working Papers on Operations Management*, 2(1), 18–30.
- Grangier, P., Gendreau, M., Lehuédé, F., & Rousseau, L. M. (2016). An adaptive large neighborhood search for the two-echelon multiple-trip vehicle routing problem with satellite synchronization. *European Journal of Operational Research*, 254(1), 80–91.
- Hemmelmayr, V. C., Cordeau, J.-F., & Crainic, T. G. (2012). An adaptive large neighborhood search heuristic for two-echelon vehicle routing problems arising in city logistics. *Computers & Operations Research*, 39(12), 3215–3228.
- Hof, J., Schneider, M., & Goeke, D. (2017). Solving the battery swap station location-routing problem with capacitated electric vehicles using an avns algorithm for vehicle-routing problems with intermediate stops. *Transportation Research Part B: Methodological*, 97, 102–112.
- Irnich, S., & Desaulniers, G. (2005). Shortest path problems with resource constraints. In *Column generation* (pp. 33–65). Springer.
- Jacobsen, S. K., & Madsen, O. B. (1980). A comparative study of heuristics for a two-level routing-location problem. *European Journal of Operational Research*, 5(6), 378–387.
- Jepsen, M., Spoorendonk, S., & Ropke, S. (2013). A branch-and-cut algorithm for the symmetric two-echelon capacitated vehicle routing problem. *Transportation Science*, 47(1), 23–37.
- Jin, M., Liu, K., & Eksiloglu, B. (2008). A column generation approach for the split delivery vehicle routing problem. *Operations Research Letters*, 36(2), 265–270.
- Kim, L. (2011). Namsan electric bus cruises into international lime-light. <http://www.cnn.go.com/seoul/life/namsan-electric-bus-cruises-lime-light-262862/>.
- Laporte, G., Musmanno, R., & Vocaturro, F. (2010). An adaptive large neighbourhood search heuristic for the capacitated arc-routing problem with stochastic demands. *Transportation Science*, 44(1), 125–135.
- Li, H., Liu, Y., Jian, X., & Lu, Y. (2018). The two-echelon distribution system considering the real-time transshipment capacity varying. *Transportation Research Part B: Methodological*, 110, 239–260.
- Li, H., Yuan, J., Lv, T., & Chang, X. (2016a). The two-echelon time-constrained vehicle routing problem in linehaul-delivery systems considering carbon dioxide emissions. *Transportation Research Part D: Transport and Environment*, 49, 231–245.
- Li, H., Zhang, L., Lv, T., & Chang, X. (2016b). The two-echelon time-constrained vehicle routing problem in Linehaul-delivery systems. *Transportation Research Part B: Methodological*, 94, 169–188.
- Li, J. Q. (2014). Transit bus scheduling with limited energy. *Transportation Science*, 48(4), 521–539.
- Liao, C.-S., Lu, S.-H., & Shen, Z.-J. M. (2016). The electric vehicle touring problem. *Transportation Research Part B: Methodological*, 86, 163–180.
- Lin, S. W., Yu, V. F., & Chou, S. Y. (2009). Solving the truck and trailer routing problem based on a simulated annealing heuristic. *Computers & Operations Research*, 36(5), 1683–1692.
- NHTSA (2016). EPA and DOT finalize greenhouse gas and fuel efficiency standards for medium- and heavy-duty engines and vehicles. <https://westransnews.org/2016/08/epa-and-dot-finalize-greenhouse-gas-and-fuel-efficiency-standards-for-medium-and-heavy-duty-engines-and-vehicles/>.
- Pelletier, S., Jabali, O., & Laporte, G. (2016). 50th anniversary invited article-goods distribution with electric vehicles: review and research perspectives. *Transportation Science*, 50(1), 3–22.
- Perboli, G., & Tadei, R. (2010). New families of valid inequalities for the two-echelon vehicle routing problem. *Electronic notes in discrete mathematics*, 36, 639–646.
- Perboli, G., Tadei, R., & Vigo, D. (2011). The two-echelon capacitated vehicle routing problem: Models and math-based heuristics. *Transportation Science*, 45(3), 364–380.
- Pisinger, D., & Ropke, S. (2007). A general heuristic for vehicle routing problems. *Computers & Operations Research*, 34(8), 2403–2435.
- Prins, C., Prodhon, C., & Wolfier-Calvo, R. (2004). Nouveaux algorithmes pour le problème de localisation et routage sous contraintes de capacité. In *Mosim: Vol. 4* (pp. 1115–1122).
- Prodhon, C., & Prins, C. (2014). A survey of recent research on location-routing problems. *European Journal of Operational Research*, 238(1), 1–17.
- Ribeiro, G. M., & Laporte, G. (2012). An adaptive large neighborhood search heuristic for the cumulative capacitated vehicle routing problem. *Computers & Operations Research*, 39(3), 728–735.
- Ropke, S., & Pisinger, D. (2006a). An adaptive large neighborhood search heuristic for the pickup and delivery problem with time windows. *Transportation science*, 40(4), 455–472.
- Ropke, S., & Pisinger, D. (2006b). A unified heuristic for a large class of vehicle routing problems with backhauls. *European Journal of Operational Research*, 171(3), 750–775.
- Ryan, D. M., & Foster, B. A. (1981). An integer programming approach to scheduling. *Publication of Elsevier Science Publishers Bv*, 1, 269–280.
- Santos, F. A., da Cunha, A. S., & Mateus, G. R. (2013). Branch-and-price algorithms for the two-echelon capacitated vehicle routing problem. *Optimization Letters*, 7(7), 1537–1547.
- Santos, F. A., Mateus, G. R., & da Cunha, A. S. (2014). A branch-and-cut-and-price algorithm for the two-echelon capacitated vehicle routing problem. *Transportation Science*, 49(2), 355–368.
- Savelsbergh, M., & Woensel, T. V. (2016). 50th anniversary invited article!“city logistics: Challenges and opportunities. *Transportation Science*, 50, 579–590.
- Schiffer, M., & Walther, G. (2017a). An adaptive large neighborhood search for the location-routing problem with intra-route facilities. *Transportation Science*, 52(2), 331–352.
- Schiffer, M., & Walther, G. (2017b). The electric location routing problem with time windows and partial recharging. *European Journal of Operational Research*, 260(3), 995–1013.
- Schneider, M., Stenger, A., & Goeke, D. (2014). The electric vehicle-routing problem with time windows and recharging stations. *Transportation Science*, 48(4), 500–520.
- Schwengerer, M., Pirkwieser, S., & Raidl, G. R. (2012). A variable neighborhood search approach for the two-echelon location-routing problem. In *European conference on evolutionary computation in combinatorial optimization* (pp. 13–24).
- Shaw, P. (1998). Using constraint programming and local search methods to solve vehicle routing problems. In *Principles and practice of constraint programming CP* (pp. 417–431). Springer.
- UPS (2015). UPS expands electric vehicle fleet in texas. <http://www.postaltechnologyinternational.com/news.php?NewsID=74415>.
- Villegas, J. G., Prins, C., Prodhon, C., Medaglia, A. L., & Velasco, N. (2013). A matheuristic for the truck and trailer routing problem !. *European Journal of Operational Research*, 230(2), 231–244.
- Villegas, J. G., Prins, C., Prodhon, C., & Velasco, N. (2011). A GRASP with evolutionary path relinking for the truck and trailer routing problem. *Computers & Operations Research*, 38(9), 1319–1334.
- Yang, J., & Sun, H. (2015). Battery swap station location-routing problem with capacitated electric vehicles. *Computers & Operations Research*, 55, 217–232.
- Zhang, Q., Wu, L., Yang, Z., Zou, C., Liu, X., Zhang, K., et al. (2016). Characteristics of gaseous and particulate pollutants exhaust from logistics transportation vehicle on real-world conditions. *Transportation Research Part D Transport & Environment*, 43, 40–48.